OPTIMAL POWER ALLOCATION FOR ENERGY EFFICIENT MIMO RELAY SYSTEMS IN 5G WIRELESS COMMUNICATION

Md R. U. D. Rajib

A Thesis

in

The Department

of

Department of Electrical and Computer Science

Presented in Partial Fulfillment of the Requirements

for the Degree of

Master of Applied Science (Electrical and Computer Engineering) at

Concordia University

Montréal, Québec, Canada

May 2018

CONCORDIA UNIVERSITY

School of Graduate Studies

This is to certify that the thesis prepared

By: **Md R. U. D. Rajib**

Entitled: **OPTIMAL POWER ALLOCATION FOR ENERGY EFFICIENT MIMO RELAY SYSTEMS IN 5G WIRELESS COMMUNICATION**

and submitted in partial fulfillment of the requirements for the degree of

Master of Applied Science (Electrical and Computer Engineering)

complies with the regulations of this University and meets the accepted standards with respect to originality and quality.

Signed by the Final Examining Committee:

_____ Chair
Dr. Dongyu Qiu

_____ External Examiner
Dr. Arash Mohammadi (CIISE)

_____ Examiner
Dr. Omair Ahmad

_____ Supervisor
Dr. Wei-Ping Zhu

Approved by _____
Dr. W. E. Lynch, Chair
Department of Department of Electrical and Computer Science

_____ 2018

_____
Dr. Amir Asif, Dean
Faculty of Engineering and Computer Science

Abstract

OPTIMAL POWER ALLOCATION FOR ENERGY EFFICIENT MIMO RELAY SYSTEMS IN 5G WIRELESS COMMUNICATION

Md R. U. D. Rajib

Wireless communication has undergone a significant growth to meet the unexpected demand of wireless data traffic over the past two decades. As manifested by the revolution of the third and fourth generations and long-term evolution advanced (LTE-A), engineers and researchers have been devoted to the development of the next-generation (5G) wireless solutions to meet the anticipated demand of 2020. To this end, cooperative relay communication has been introduced as an enabling technology to increase the throughput and extend the coverage of the broadband wireless networks. Decode-and-forward (DF) has been known as an effective cooperative relaying strategy for its outstanding features. On the other hand, merging massive multi-input-multi-output (MIMO) with cooperative DF relay is considered as a key technology for 5G wireless networks to improve the quality-of-service (QoS) in a cost-effective manner. The objective of this thesis is to establish and solve a power allocation optimization problem for energy efficient multi-pair DF relay systems integrated with massive MIMO.

The first part of the thesis is focused on a constrained optimization problem to minimize the total transmit power for each transmission phase of the DF relay. Due to the non-convexity characteristic, the objective function is approximated as a convex function by means of complementary geometric programming (CGP) which is then solved by a sequence of geometric programming (GP). A lower bound of average SINR is also introduced by adopting the MMSE channel state information (CSI) to relax the constraint functions in the standard GP form. Finally, we proposed a homotopy or continuation method based algorithm to solve the optimization problem via popular CVX optimization toolbox. MATLAB simulations are conducted to validate the proposed algorithm.

In the second part, another optimization problem is presented for the entire two-hop transmission of the DF relay to improve the global energy efficiency (GEE) under different channel conditions. Here, we estimate the channel by maximum likelihood (ML) criterion and investigate a closed-form expression of GEE. Further, GEE is approximated in a convex form by applying CGP due to the difficulty arising from the non-convexity and a lower bound of the average SINR expression is also derived to relax the constraint functions in the GP problem. Numerical results showing a detailed comparison of GEE under ML and MMSE channel estimation conditions and the performance improvement from the proposed algorithm are provided.

Acknowledgements

I would like to start with my appreciation and sincerest gratitude to my supervisor, Prof. Wei-Ping Zhu. I have benefited tremendously from countless interactions and discussions with him. His emphasis on the fundamental nature of techniques and problems inspired many aspects of this thesis. His precise and thorough approach to research has set up an example that I wish to follow in my future career. He also deserves many, many thanks for carefully reading my manuscripts and patiently improving my English writing.

I would like to give special thanks to Prof. Wassam Ajib, Universit du Qubec a Montral, Canada for his support, valuable comments and suggestions in my research activities. I am grateful to my colleagues and friends, Mr. Ali Mohebbi, and Mr. Md Manik Mia, and all my signal processing laboratory members for their assistance, friendship, and cooperation.

I am also grateful to Concordia University for providing me with the GSSP funding and split scholarship during my M.A.Sc study. At last but not the least, I am forever indebted to my parents and sisters for their support throughout my entire life. I hope to have something better than this thesis to dedicate to them in the future.

Contents

List of Figures

List of Tables

List of Symbols

S	Source
D	Destination
R	Relay system
N	Number of user interfaces
S_n	Number of source user interfaces
D_n	Number of destination user interfaces
M	Relay antennas
T_c	Coherence time
B_c	Coherence bandwidth
B	Total bandwidth
τ_c	Coherence interval
τ_{sp}	Pilot symbols (source)
τ_{dp}	Pilot symbols (relay)
τ_{sn}	Data symbols (source)
τ_{dn}	Data symbols (relay)
$\mathbf{H}$	Channel matrix
$\mathbf{H}_s$	Channel matrix (source to relay)
$\mathbf{H}_d$	Channel matrix (relay to destination)
$\mathbf{D}_s$	Small scale fading (source to relay)
$\mathbf{D}_d$	Small scale fading (relay to destination)

$\mathbf{G}_s$	Large scale fading (source to relay)
$\mathbf{G}_d$	Large scale fading (relay to destination)
ζ	Number of diagonal matrix of $\mathbf{G}$
$\mathbf{X}_p$	Transmit pilot signals
$\mathbf{Y}_p$	Received pilot signals
$\mathbf{W}_p$	Noise signals (pilot)
$\mathbf{P}_p$	Pilot power
σ_{sn}	Variance of estimated channel (relay)
σ_{dn}	Variance of estimated channel (destination)
ξ_{sn}	Variance of estimated error (relay)
ξ_{dn}	Variance of estimated error (destination)
$\mathbf{I}$	Identity matrix
$\hat{\mathbf{H}}$	Channel estimation
$\overline{\mathbf{H}}$	Channel estimation error
$\mathbf{s}$	Transmitted data signals
$\mathbf{y}_r$	Received data signals at relay
$\mathbf{P}_s$	Power allocation matrix (source)
$\mathbf{P}_d$	Power allocation matrix (relay)
$\mathbf{w}_r$	Noise vector at relay
$\mathbf{w}_d$	Noise vector at destination
$\hat{\mathbf{y}}_r$	Estimated data signals at relay
$\mathbf{F}_s$	Processing matrix for detection
$\mathbf{F}_d$	Processing matrix for transmission
γ_{sn}	SINR for source to relay (MRC)
γ_{dn}	SINR for relay to destination (MRT)
R_{MRC}	MRC sum-rates
R_{MRT}	MRT sum-rates

EE_{MRC}	MRC energy efficiency
EE_{MRT}	MRT energy efficiency
P_{st}	Total power for source to relay
P_{dt}	Total power for relay to destination
P_{tt}	Total power for all phases
P_s^{max}	Maximum power for each user (source)
P_d^{max}	Maximum power for each user (relay)
P_p^{max}	Maximum pilot power
$[.]^T$	Transpose operation
$E[.]$	Expected value

List of Abbreviations

5G	Fifth generation
AF	Amplify-and-forward
AWGN	Additive white Gaussian noise
BER	Bit error rate
CCI	Co-channel interference
CGP	Complementary geometric programming
CSI	Channel state information
DF	Decode-and-forward
EE	Energy efficiency
FG	Fixed gain
GEE	Global energy efficiency
GP	Geometric programming
LP	Linear programming
LSF	Large scale fading
MIMO	Multi-input-multi-output
ML	Maximum likelihood
MMSE	Minimum mean square error
MRC	Maximum ratio combining
MRT	Maximum ratio transmission
QoS	Quality of service

RF	Radio frequency
R-D	Relay to destination
S-R	Source to relay
SE	Spectral efficiency
SINR	Signal to noise ratio
SSF	Small scale fading
TDD	Time division duplex
UEs	User interfaces
VG	Variable gain

Chapter 1

Introduction

1.1 Background Information

Wireless technologies have undergone a remarkable growth over the last decades. With the fast deployment and commercial operation of 4G systems, technologists worldwide have been devoted to explore next-generation wireless solutions to meet the anticipated demand in the 2020 era for the explosive growth of data traffic [1]. For instance, wireless data traffic demand increases dramatically due to cellular systems, data networks and wireless local area networks (WLAN) for business, home, and environmental applications. Also, a lot of new services are fast emerging including e-health, e-banking, e-learning, and so on [2]. This exponential growth of data traffic and the demand for ubiquitous connectivity have given rise to a serious carbon emission problem and made communication technologies very challenging [2], [3]. Hence, telecommunication researchers and engineers are currently working towards 5G wireless communication systems to design energy efficient wireless network architectures to address the aforementioned future technical challenges. Therefore, energy efficiency (EE) has been accepted as an important design metric of 5G mobile communication systems [1], [4]-[5].

1.1.1 Fundamental Concepts of MIMO Relaying

One of the fundamental challenges of wireless communication is the low reliability of wireless channels. This pertains to the channel impairment due to multipath, fading, and shadowing, which

is caused by receiving different versions of the source signal from different paths. The propagation paths result from scattering, reflection, and diffraction of the transmitted signals by objects in the environment [6], such as buildings, trees, etc. Therefore, the capacity of a wireless channel has a high variability.

In conventional techniques, the wireless channels are exploited in time and frequency dimensions for increasing data rate, enhancing link-reliability, and reducing energy consumption [7]. Nevertheless, these techniques are approaching their fundamental limits or providing only marginal performance improvements. Meanwhile, the spectrum resource over a wireless channel is limited, and the required spectrum has increased as a consequence of large demand of high data rate services. Therefore, the use of the limited frequency resource to satisfy the quality of service (QoS) requirements has restricted the cellular coverage. The traditional techniques of extending coverage and improving the data rates include network densification which is to deploy more base stations to serve in smaller cells. Nevertheless, this approach in effect drives up deployment cost significantly. As a remedy to this problem as well as to circumvent the challenge in next-generation wireless networks, cooperative relaying has been developed [8], [9]. Cooperative relaying is to extend the coverage of a base station (BS) by deploying single or multiple relay stations around BS [8]. It has already been accepted by several standards, e.g., IEEE 802.11s, IEEE 802.16j, and LTE-A as a promising technique to expand the coverage, reduce the power consumption and achieve energy-efficient transmission [9]. There is another technology called very large scale antenna array or massive MIMO which has been identified as one of the efficient technology directions for fifth generation (5G) wireless standards [10]. Merging the massive MIMO with cooperative relaying is considered as a new wireless architectural design which plays a key role for next-generation wireless standards. It is developed to meet the unprecedented increasing demand for faster, reliable and seamless wireless connectivity.

The concept of transmitting a signal between two communication terminals using a relay system (R) has first appeared in the year 1970 [11]. However, relay systems came into focus only in the last decades as employed in multi-carrier relay and next-generation wireless communication, where relay nodes receive the source signal and re-transmit it to the destination based on some protocols. Relays can be mobile terminals (user terminals) or fixed terminals known as infrastructure relays.

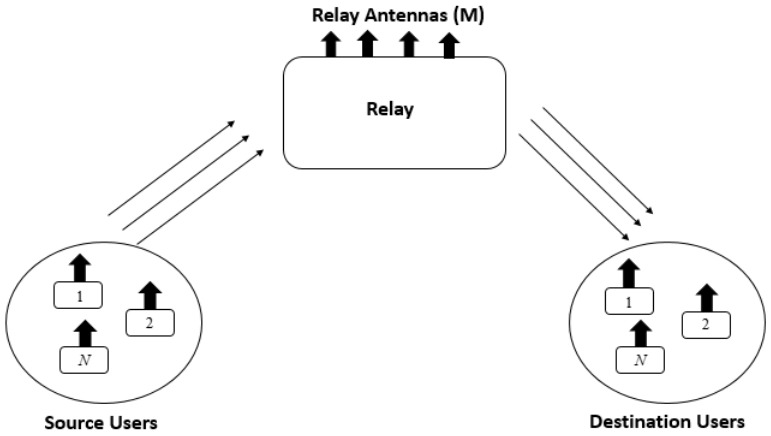

Figure 1.1: Two-hop relay system.

When there is only one relay node assigned to cooperate the communication between the source and the destination, it is called a two-hop single-relay system. In a two-hop one way relaying communication system as shown in Figure 1.1, the general operation can be divided into two phases. In the first phase, the source (S) transmits the signal to the relay node if there is no direct connection between source to destination. During the second phase, the relay forwards the received signal to the destination (D) node through an orthogonal (non-interfering) channel, while the source keeps silent. The destination node received the signals transmitted from relay system and combined the signals to improve the signal to interference plus noise ratio (SINR).

The single-antenna relay networks are capable of expanding coverage and enhancing the link reliability, but they may not be able to increase the data rates. Multiple-antenna or MIMO relay networks are the natural generalization of single antenna relay network for multiple-antenna terminals [12], [13]. In MIMO relaying, the spatial dimension of the wireless channels is exploited by sending multiple-streams of data signals via multiple-antennas over multiple-relayed hops. Thus, MIMO relay networks can simultaneously benefit from relaying and MIMO technology. Specifically, MIMO relaying can provide some unique benefits, which would not necessarily be achieved by using either relay or MIMO technology separately. For instance, MIMO relay networks can provide diversity against large-scale fading or shadowing, which cannot be mitigated purely with colocated antennas. Due to these advantages, MIMO relaying techniques have recently gained significant research

interest and are being investigated for emerging next-generation wireless standards [14], [15].

1.1.2 Classification of Relay Schemes

A variety of relay schemes have been proposed as systematically reviewed in [16]. According to the processing functionality of relay node, the cooperative communication scheme can be divided into two major categories:

- Transparent relaying techniques
- Regenerative relaying techniques

Transparent relaying techniques

In this approach, the relay system mainly performs simple power scaling and/or phase rotation, i.e., a linear transformation of a signal received at relay. Among the transparent techniques, amplify-and-forward (AF) attracts most of the attention in relay system considerations. One of the key parameters in AF relaying design is the amplifying gain. There are two widely used types of amplifying gains such as variable gain and fixed gain. Variable gain depends on the instantaneous channel fading of the received path to choose the amplification gain, and fixed gain is constant and depends on the fading channel statistics [17]. In AF relaying, relay system receives a signal from the source, amplifies it either with a fixed gain (FG) or a variable gain (VG) and then forwards it to the destination.

Regenerative relaying techniques

This technique includes alternation of a signal waveform and/or its information content, i.e., the nonlinear transformation of a signal received at relay system. Decode-and-forward (DF) is a typical example of the regenerative relaying technique. In DF scheme, the relay implements a full physical layer transceiver. It decodes the signals received from the source, re-encodes the entire received signal, and then re-transmits it to the destination. In order to achieve the maximal diversity, the relay should be able to know whether or not it has decoded correctly and then transmit the re-encoded

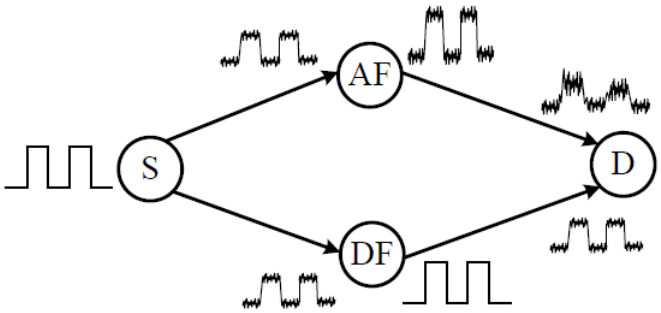

Figure 1.2: Comparison of the signal processing between AF and DF relays.

signal based on the obtained knowledge. Under reasonable channel conditions, the regenerated signal can be identical to the source signal.

Figure 1.2 compares the signal processing in AF and DF relays. As illustrated in Figure 1.2, DF relay can generate the clean re-transmitted signal which is equal to the signal transmitted by the source. In contrast to DF relay, the noise and fading of the two-hop channel is accumulated with the desired signals along the transmission path in the AF relay systems. AF relay forwards the decoded signals blindly and the system performance is usually degraded by errors at the relay which are propagated to the destination. The DF relay ability of transmitting a clean signal can be realized through some sophisticated mechanisms, such as error detecting codes [18] and appropriate SINR thresholds at the relay [17], which increased the complexity of the systems. However, applying proper beamforming matrix and using channel estimation techniques can help to figure out the error propagation and improve the system performance.

Relay schemes can also be clarified as one-way and two-way systems. In one-way relay systems, the information is always transmitted from the source node, and the destination only receives the signal of the source. In two-way scenario, the communication is bidirectional where two users exchange information. Under this scenario, each node is not only a source, but also the intended destination of the other node. Examples of two-way relay systems are when a mobile user communicates with the BS via a dedicated relay in a cellular system, or two mobile users exchange their data in a WLAN via the access point.

1.2 Literature Review

The concept of cooperative communication can be traced back to the three-terminal communication channel (or the relay channel) [19]. Upper and lower bounds on the capacity of such channel were also developed in [19]. Shortly thereafter, Cover and El Gamal studied the general relay channel and established an achievable lower bound for data transmission [8]. These two seminal works laid down the foundation for nowadays research on cooperative relay communication. Most recently, applying MIMO techniques to relay communication [12] has been also under consideration as it gradually increases the demand of research day by day.

The MIMO technology is maturing and is being integrated into emerging wireless broadband standards like long-term evolution LTE-A [20]. For example, LTE-A standard allows for up to eight antenna ports at BS. As a matter of fact, the more antennas are equipped at BS, the more degrees of freedom that the propagation channel can provide an outstanding performance. This concept drives the next generation wireless communication toward massive MIMO [10]. Massive MIMO proposes utilizing a very high number of antennas to multiplex messages for several devices on each time-frequency resource, focusing the radiated energy toward the intended directions while minimizing interferences. It has attracted considerable attention due to its potential for achieving substantial spectral efficiency (SE) and EE [21], [22].

The energy-efficient design of massive MIMO systems has emerged as a new research trend for future wireless communications [22]. Basically, resource allocation (RA) is the primary goal for EE. RA aim to maximize the end-to-end channel capacity or minimize the resource consumption by allocating system and channel resources, including time slots, frequency bandwidth, power consumption etc. For example, a realistic power consumption model is proposed in [23] that provides optimal system parameters for maximizing EE in a multi-user massive MIMO system. Further, merging massive MIMO and cooperative relaying is an appealing option for future energy efficient cellular networks [12]. It was shown in [24], [25] that using simple relay transceivers, a multi-antenna relay system is capable of significantly alleviating the interference among different data streams/user equipments (UEs). RA also plays a crucial role in relay networks. In [26], the channel resource is allocated by maximizing the instantaneous channel capacity subject to the total power

constraint in a two-hop relay system. The authors also proposed in [27] that the capacity is maximized for individual power constraints by allocating channel resources. Similar observations are identified in single-hop relay equipped with massive MIMO. It was shown in [28] that SE of a relay equipped with a large-scale antenna array and a zero forcing (ZF) transceiver is proportional to the number of relay antennas, leading to a huge amount of SE increase as compared with a single antenna relay system.

The existing works on massive MIMO aided relay systems are mainly focused on analyzing the throughput performance limits in various specific system configurations [29]-[31] and designing RA for improving the throughput performance in different contexts [32]-[34]. For instance, the asymptotic SE performance of massive MIMO aided multi-pair two-way relay systems were investigated in [29], [30]. The asymptotic results are beneficial to provide more insightful understandings of very large antenna system to eliminate the inter-pair interference and reduce the total power consumption. The SE and EE performance limits in massive MIMO aided multi-pair full-duplex relay systems were also studied in [31]. The authors provide the available regions where full-duplex systems can outperform half-duplex systems to increase the EE performance based on the practical power consumption model. As a consequence, the authors in [32] considered the peak power constraints and the rate requirements of each individual user pair and proposed a computationally efficient optimal power allocation algorithm for minimizing the overall power consumption of a massive MIMO aided multi-pair full-duplex DF relay system. Additionally, in [33], [34], a low complexity power control scheme was conceived for optimizing SE and EE of massive MIMO aided full duplex AF relay systems. Three power allocation schemes were proposed in [35]-[37] for maximizing SE of a massive MIMO aided multi-pair two-way AF relay system under different sets of constraints. Note that in most of the aforementioned studies SE is used as the performance metric which characterizes the systems throughput. Although the EE performance limits have indeed been analyzed for massive MIMO aided multi-pair full-duplex relay systems in [31]-[33], to the best of our knowledge, there is a scarcity of research investigating the power allocation for maximizing the EE of massive MIMO relay systems. The main reason is that the energy-efficient power allocation has to consider both the systems SE and total power consumption, and the resultant problem is a complicated optimization problem, which is often non-convex and thus difficult to solve as

compared with the power allocation for maximizing SE only.

1.3 Motivation and Objectives

From the aforementioned brief literature review, a ton of works had already been done in analyzing RA, increasing throughput performance, and SE. There are several challenges in attempts to provide high-quality service in wireless environment. Large efforts have been made in the investigation and implementation of wireless communication systems to accommodate communication reliability, coverage, and high data rate services for various applications. Different power consumption models and different types of relay models like half-duplex or full-duplex AF relay merging with massive MIMO have been studied for energy efficient wireless communication. Many researchers have provided effective solutions for the channel impairment due to multipath, fading, and shadowing. However, there is a huge gap between the growth rates of wireless data traffic demand and capacity growth rates of present wireless access technologies.

As a consequence, there are many challenges in the reliability and efficiency of the system in multi-hop relay transmission, although the relay technology is promising in improving communication quality. Most of the recent works have focused on MIMO aided AF relay systems. AF is the most useful one which can be characterized by simpler realization and less delay introduced at relay stations. On the other hand, it holds a significant disadvantage in the sense that amplifying a signal would amplify the present noise as well. In AF, the relay simply captures the waveform received from the source, amplifies it, and then re-transmits a noisy version of the source signal to the destination. Another major challenge of this cooperative communication is the low transmission reliability due to the channel characteristic of the transmission links (i.e., S-R link, and R-D link). In non-coherent cooperative relay systems, the channel condition will become worse because of the accumulation of multipath fading in the multiple hops if there are no channel compensation techniques at relay nodes. However, without channel compensation techniques at AF relay nodes, the severe channel response will increase the noise level in the system, and cause the reduction of the transmission reliability of the relay link [38], [42]. But in the case of regenerative relaying, DF

relaying has a specific advantage as it completely separates optimization of S-R and R-D connections. In DF, the process of re-encoding in the relay node could be completed with a code which is the most adequate for R-D link no matter what code was used for the signal transmission over S-R link.

The authors in [43] investigated power allocation optimization for global energy efficiency (GEE) maximization in massive MIMO for one-way DF relay systems. A non-convex power allocation optimization problem with the objective of GEE maximization is formulated under specific QoS and transmit power constraints and is solved by converting the original optimization problem into a convex one using the successive convex approximation techniques. But the system is considered more complex than the direct combination of different transmission phases like S-R and R-D. Therefore, the main objective of this thesis is to solve a challenging power allocation optimization problem for the join and individual transmission phase of the DF relay system equipped with massive MIMO by using numerical convex optimization techniques.

1.4 Contributions of the Thesis

The above mentioned issues and factors encourage us to investigate the massive MIMO relay communication systems and propose solutions for maximizing EE and GEE for next-generation wireless communication. Specifically, motivated by the benefits of massive MIMO relaying, we investigate energy-efficient power allocation optimization strategies in a massive MIMO aided multi-pair one-way DF relay system, where N pairs of users exchange messages with each other via a common relay which is equipped with large-scale antennas. We assume channel state information (CSI) is estimated based on the minimum mean square error (MMSE) and maximum likelihood (ML) criterion [44], and the relay system employs maximum ratio combining/maximum ratio transmission (MRC/MRT) beamforming to process the signals.

- An accurate closed-form expression of EE is derived for each transmission phase for a massive MIMO aided multi-pair DF relay system, where the data rates of both transmission phases have to be matched with each other. An optimization problem is established to maximize the

EE subject to transmitting power and SINR constraints. Because the objective function is a rational function and very difficult to solve, a successive convex approximation sub-problem for power allocation is formulated by applying complementary geometric programming (CGP) [45], [46]. Next, a lower bound SINR expression [47] is adopted to transform the SINR constraints function to standard geometric programming (GP) [48], which can be solved efficiently by convex optimization tools, such as CVX [49]. Finally, an algorithm is designed for each transmission phase (i.e., S-R link and R-D link) based on homotopy [50] together with CGP and GP to perform optimal power allocation for maximizing the EE gains.

- We addressed the GEE issue based on the same system model and showed a detail comparison under different channel conditions, namely, MMSE and ML channel conditions. Here GEE is calculated from total sum-rates divided by the total power consumption. At the beginning, we estimated the channel under ML criterion and derived an accurate closed-form expression of GEE to formulate GEE maximization problem. A successive convex approximation sub-problem for power allocation is formulated and a lower bound SINR expression is applied to transform the SINR constraints function into the standard GP format. Lastly, two algorithms are designed for MMSE and ML channel condition based on homotopy together with CGP and GP to improve the GEE performance. Simulation results are provided to demonstrate the EE and GEE performance of this DF relay system model.

1.5 Organization of the Thesis

The rest of this thesis is formed as follows:

Chapter 2: This chapter first briefly discusses relaying techniques for massive MIMO. A basic system model of multi-pair one-way massive MIMO aided DF relay is presented, showing antenna configuration, CSI acquisition, and transmission frame structure. A practical channel model is also discussed in the context of massive MIMO, together with MMSE channel estimation. Then, the processing of signals in each transmission phase using MRC/MRT linear processing techniques is briefly reviewed. Closed-form expressions of EE for all transmission links are derived at the remainder of this chapter.

Chapter 3: A general optimization problem for EE maximization is then formulated based on convex optimization criteria. Due to the non-convexity characteristic of the problem, some necessary convex optimization methods are briefly described to reformulate the optimal power allocation problem. First, we show that EE maximization problem is equivalent to CGP. Then, the optimization problem is reformulated as a successive convex approximation sub-problem. A lower bound of SINR expression is derived to transform the SINR expression into a standard GP so that it can be easily solved by CVX tool. Finally, two algorithms are proposed to obtain the optimal power for maximizing EE for S-R and R-D transmission phases. MATLAB simulations are conducted to validate the proposed algorithms.

Chapter 4: This chapter shows the GEE performance under different channel estimation conditions of the massive MIMO multi-pair DF relay system. We first investigate the signal processing under equal power allocation in both phases and derive the closed form expression for GEE. An optimization problem is proposed to maximize the GEE and reformulated in convex form using some numerical optimization methods. Finally, two algorithms are designed to show the GEE performance under MMSE and ML channel estimation conditions, through MATLAB simulations.

Chapter 5: The conclusions of the thesis are summarized. Some future research directions relevant to the work in this thesis are also discussed.

Chapter 2

Massive MIMO Aided Relay Configuration

2.1 Introduction

It is well known that signal fading arising from multipath propagation can be mitigated through the use of diversity. Diversity in a wireless system provides several copies of the transmitted signal to the destination node, which can be achieved through time, frequency, and spatial diversity. The most popular technique to achieve spatial diversity is the massive MIMO system. This technique is already identified as most attractive one for its significant improvement to information rate and transmission reliability [10]. Massive MIMO enables an aggressive spectral multiplexing technique and achieves an unbelievable SE. It utilizes a very large number of antennas for steering wireless signals among multiple spatially distributed user nodes. Specifically, very large antenna arrays can be formed to concentrate radio frequency (RF) signals towards intended directions by using transmit beamforming techniques and thereby minimize the co-channel interferences (CCI)[12], [14]. It has been predicted that massive MIMO can achieve a goal of 5 to 15 times SE improvement compared to the existing technologies [7]. Another prominent benefit of massive MIMO is the unprecedented gain in EE, which is obtained by focusing the radiated energy on smaller regions of space with extreme sharpness [10], [12]. In particular, massive MIMO in wireless network enables a drastically less output RF power than that of the current technology for the substantial EE gain [22]. Therefore,

not only the total energy consumption but also the CO_2 emissions can be reduced. In this manner, green and environment-friendly wireless technology can be designed for next-generation wireless communication [1], [4]. For this basis, the International Telecommunication Union has proposed this technology as one of the 5G requirement [10].

One of the key architectural design challenges of massive MIMO systems is to accommodate a very large number of antennas, transceivers and associated power amplifiers in a space-limited BS. Nevertheless, as a consequence of the recent research advances in mmWave wireless communication techniques, massive MIMO has increasingly become practically viable. High cost and complicated implementation issues bring challenges to MIMO systems. Interestingly, relaying techniques can be further generalized by massive MIMO technology, and the corresponding new wireless architectural design is anticipated to take a central part in advancing the emerging next-generation wireless standards [7]. Relay communication is a specific kind of wireless cooperative communication, which has been demonstrated to be an effective way to combat wireless fading by merging with multi-antenna configurations. It has recently become a key technology for the modern wireless networks as an effective means of saving power, attaining broader coverage range, and mitigating channel impairments resulting from fading [12]. The application of relays in cellular systems permit economical design for the case that there are few or infrequent users at the edge of cellular. Since the relay does not need a wired connection to the backhaul, it can eliminate the costs that serves as the interface between the BS and the wired backhaul network. Besides, relay communication reduces the required transmit power compared to those for a BS due to the smaller coverage. Moreover, the propagation loss from the relay to a terminal is much lower than that from a BS to the terminal, which ensures higher data rates in larger cells [13].

In this thesis, a massive MIMO aided multi-pair one-way DF relay system is considered where N pairs of user interfaces (UEs) communicate with each other via a relay that is equipped with a large-scale antenna array [43]. In this system, the source sends the pilot signal to relay to capture CSI and then sends the appropriate data signal to relay. Relay system first decodes the signal and determines the presence of errors. If the received signal is decoded with no errors, pilot signal is sent again to find the proper destination. Finally, it sends the data signal to the appropriate destination. This is a universal and fundamental model for many wireless communication scenarios.

For instance, it can characterize a macro cellular system where the macro BS acts as the relay and rate matching is imposed in the uplink/downlink. It can also describe a mmWave based small-cell sub-system of a heterogeneous cellular system that is composed of a macro cell and several small cells. BS of each small cell is responsible for linking the users in its vicinity. These small cells are normally deployed in some areas having extremely high traffic, or in the border area of a macro cell to reduce the impact of path loss or of the shadowing fading caused by large obstacles between the source UEs and the destination UEs. Likewise, it can also be invoked to characterize a cluster of a hierarchical multi-hop ad-hoc network, where the relay acts as the cluster head. A large number of antennas can be installed on relays by using high-frequency band and more compact 2-D and 3-D antenna arrays. More information about multi-pair relay systems can be found in [25], [28], [32].

2.2 System Architecture

A schematic diagram of the massive MIMO aided multi-pair one-way DF relay is depicted in Figure 2.1. In this system model, N single-antenna source UEs S_n, or $n = 1, \cdots, N$ are simultaneously transmit their signals to the corresponding N single-antenna destination UEs D_n, via a shared relay equipped with M antennas. The system operates over a bandwidth of B Hz and each UE as well as the relay use the whole bandwidth. All user terminals are single-antenna nodes, whereas the relay is a multiple-antenna terminal. There are no direct links between source and destination due to large-scale path-loss. In general, the concept of massive MIMO is a natural generalization of the conventional multi-user MIMO. However, they differ in several ways such as

- Antenna configuration
- CSI acquisition
- Transmission frame structure

2.2.1 Antenna Configuration

In the context of massive MIMO relay networks, the number of antennas M at the relay nodes stay in between the number of user nodes of the source and destination. The benefits of using a

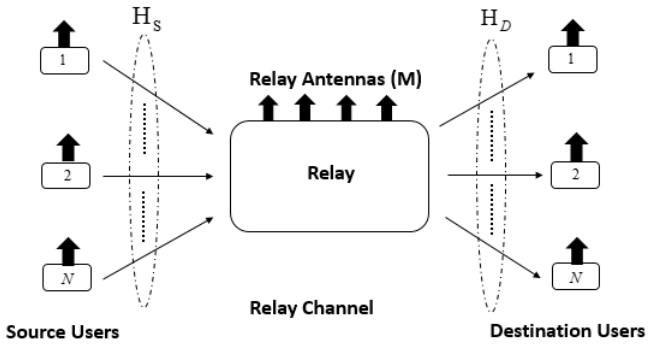

Figure 2.1: A schematic diagram of a massive MIMO aided relay network.

massive number of antennas at the relay are as follows.

- First, a large number of antennas not only offer a higher overall SE but also guarantee a uniform QoS among user nodes.
- Second, whenever M is significantly larger than N, the physical phenomenon known as channel hardening comes into play resulting in simplified signal processing at the relay.

Specifically, the small-scale fading (SSF) and the underlying frequency dependencies of wireless channels are disappeared due to channel hardening, and the corresponding performance metrics depend only on the large-scale fading (LSF) effects. Further, wireless RA and scheduling techniques become significantly less complicated.

2.2.2 Channel State Information Acquisition

The CSI acquisition of massive MIMO heavily depends on the duplexing mode [7]. Here, the relay operates in the half-duplex time division (TDD) mode. In the setting of massive MIMO, two individual channel segments such as S-R and R-D have been considered for data transmission. Whenever linear processing is demanded at the relay, S-R and R-D channels can be separately estimated by using the pilots transmitted by users and relay nodes, respectively.

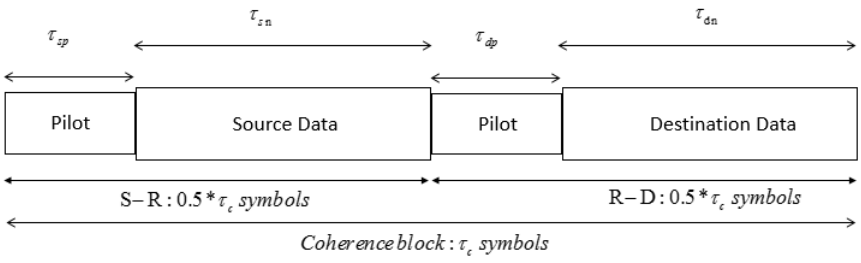

Figure 2.2: Transmission frame structure for the system model.

2.2.3 Transmission Frame Structure

The transmission frame structure for massive MIMO relay networks is defined in this subsection. The time duration in which the channel can be approximated by a time-invariant system is termed the coherence time (T_c). The frequency interval in which the channel frequency response can be approximated by a constant is called the coherence bandwidth (B_c). Then the coherence interval can be specified as the length of the time-frequency space over which the channel can be reasonably judged by a constant in both time and frequency dimensions. Hence, the coherence interval can be quantified as $\tau_c = T_c B_c$ [51] whereas the channel are static within time-frequency coherence block of symbols. In TDD mode, the channel coherence interval can be split into four segments. These segments are divided into pilot phase and S-R phase, again pilot phase and R-D phase. The ratio of the transmitted symbols are equal for both S-R and R-D, respectively. The corresponding transmission frame structure is depicted in Figure 2.2. The entire data transmission per coherence block can be expressed as

$$\tau_c = \tau_{sp} + \tau_{sn} + \tau_{dp} + \tau_{dn}. \tag{2.1}$$

Here, τ_{sp} symbols per coherence block are used as S-R pilots which should be at least equal to the number of user nodes served by the relay antenna and the τ_{dp} pilot signals are used in R-D link for the destination. The next τ_{sn} symbols per coherence block are used for transmitting payload data from the source to the relay. The remaining τ_{dn} symbols are used for the transmission of R-D payload data from the relay to the destination nodes.

2.3 Channel Propagation and Estimation

2.3.1 Channel Modeling

In this subsection, practical propagation channel models are discussed in the context of massive MIMO relay networks. The users and the antenna arrays at the relay are assumed to be settled in a dense, isotropic scattering environment. The channel matrices for S-R and R-D links are denoted by $\mathbf{H}_s$ and $\mathbf{H}_d$, respectively. Therefore, each antenna receives a superimposition of a large number of waveforms originating from independent scatterers, and $\mathbf{H}$ can be modeled as an independently distributed random matrix as follows:

$$\mathbf{H}_s = [\mathbf{h}_{s1}, \cdots, \mathbf{h}_{sN}] = \mathbf{D}_s \mathbf{G}_s^{1/2}, \tag{2.2}$$

where $\mathbf{D}_s \in C^{M \times N}$ represents the independent and identically distributed (i.i.d.) small scale fading (SSF) $CN \sim (0, 1)$. Further, $\mathbf{G}_s$ is the $N \times N$ diagonal matrix capturing large scale fading (LSF) effects such as path loss and shadowing. In this context, the channel can be described as

$$[\mathbf{H}_s]_{mn} = \sqrt{\zeta}_{sn} [\mathbf{D}]_{mn}, \quad m \in \{1, \cdots, M\}, \tag{2.3}$$

where ζ_{sn} is the nth diagonal element of $\mathbf{G}_s$ and is assumed to be independent over $m \in \{1, ..., M\}$ because the distance between the nth user node and the relay is much larger than the antenna spacing [21], [52]. Further, ζ_{sn} is assumed to be constant over many channel coherence intervals and to be known a priori as it changes very slowly with time [21]. The channel matrix between the relay and destination $\mathbf{H}_d$ can also be modeled as an independently distributed random matrix as follows:

$$\mathbf{H}_d = [\mathbf{h}_{d1}, \cdots, \mathbf{h}_{dN}]^T = \mathbf{G}_d^{1/2} \mathbf{D}_d, \tag{2.4}$$

where $\mathbf{D}_d \in C^{N \times M}$ accounts for the SSF and $\mathbf{G}_d$ is the diagonal matrix that captures LSF including the path loss and shadowing. It is assumed that the antennas at both relay and destination are co-located. Hence, the distance from any antenna pair in the relay to destination is the same. This fact can be further justified by noting that the distance between the relay and destination is far greater

than the antenna spacing. Therefore, the channel coefficient between the mth relay antenna and the nth destination nodes is denoted by

$$[\mathbf{H}_d]_{nm} = \sqrt{\zeta}_{dn}[\mathbf{D}]_{nm} \quad \text{for} \quad m \in \{1, \cdots, M\}. \tag{2.5}$$

2.3.2 Channel Estimation

The MMSE channel estimation of S-R and R-D is discussed in this subsection. Here, $\mathbf{H}_s$ and $\mathbf{H}_d$ channels are estimated at the relay and destination, respectively. By utilizing the pilots [51], a part of coherence interval is used for channel estimation. All sources transmit their pilot sequence of τ_{sp} symbols to relay and the relay node sends τ_{dp} pilot symbols to destinations. The received pilot signal at the relay can be written as

$$\mathbf{Y}_{rp} = \sqrt{\tau_{sp} p_{sp}}\mathbf{H}_s\mathbf{X}_p + \mathbf{W}_{rp}, \tag{2.6}$$

where, p_{sp} is the transmit power of each source pilot symbols and the nth row of $\mathbf{X}_p \in C^{N\times\tau_{sp}}$ is the pilot sequence transmitted from the sources. $\mathbf{W}_{rp}$ is AWGN matrices which include i.i.d $CN \sim (0, 1)$. We assume $\mathbf{X}_p\mathbf{X}_p^H = \mathbf{I}_N$ and relay system uses MMSE estimation to estimate $\mathbf{H}_s$. The MMSE channel estimate of $\mathbf{H}_s$ is given by [53]

$$\hat{\mathbf{H}}_s = \frac{1}{\sqrt{\tau_{sp} p_{sp}}}\mathbf{Y}_{rp}\mathbf{X}_p^H\overline{\mathbf{G}}_s = \mathbf{H}_s\overline{\mathbf{G}}_s + \frac{1}{\sqrt{\tau_{sp} p_{sp}}}\mathbf{W}_s\overline{\mathbf{G}}_s \tag{2.7}$$

where $\mathbf{W}_s = \mathbf{W}_{rp}\mathbf{X}_p^H$. Since the rows of $\mathbf{X}_p$ are pairwise orthogonal, the elements of $\mathbf{W}_s$ are i.i.d $CN \sim (0, 1)$ random variables. The value of $\overline{\mathbf{G}}_s$ can be described as $(\frac{\mathbf{G}_s^{-1}}{\tau_{sp} p_{sp}} + \mathbf{I}_N)^{-1}$ which is further represented by the following $\mathbf{N} \times \mathbf{N}$ diagonal matrix [47]

$$\overline{\mathbf{G}}_s = diag\left\{\frac{\zeta_{s1}}{1 + \tau_{sp} p_{sp}\zeta_{s1}}, \cdots, \frac{\zeta_{sN}}{1 + \tau_{sp} p_{sp}\zeta_{sN}}\right\} \tag{2.8}$$

Letting $\overline{\mathbf{H}}_s$ be the estimation error, the estimated channel can be decomposed by using the MMSE properties as follows

$$\mathbf{H}_s = \hat{\mathbf{H}}_s + \overline{\mathbf{H}}_s, \tag{2.9}$$

From the property of MMSE channel estimation, $\hat{\mathbf{H}}_s$ and $\overline{\mathbf{H}}_s$ are independent defined [53]. Further, we can verify the rows of $\hat{\mathbf{H}}_s$ and $\overline{\mathbf{H}}_s$ are mutually independent and distributed as $CN(0, \hat{\mathbf{G}}_s)$, and $CN(0, \overline{\mathbf{G}}_s)$ respectively. Here $\hat{\mathbf{G}}_s$ and $\overline{\mathbf{G}}_s$ are diagonal matrices whose nth diagonal elements are represented by

$$\sigma_{sn}^2 = \frac{\tau_{sp} p_{sp} \zeta_{sn}^2}{1 + \tau_{sp} p_{sp} \zeta_{sn}}, \quad \text{and} \quad \xi_{sn}^2 = \frac{\zeta_{sn}}{1 + \tau_{sp} p_{sp} \zeta_{sn}}. \tag{2.10}$$

Again, the R-D channel can be calculated at the destination by using the pilots transmitted by the relay node. Using the techniques similar to those in equation $(2.7) - (2.9)$, the MMSE estimation of the R-D channel can be deduced as follows

$$\mathbf{H}_d = \hat{\mathbf{H}}_d + \overline{\mathbf{H}}_d, \tag{2.11}$$

where $\mathbf{H}_d$ and $\overline{\mathbf{H}}_d$ are statistically independent. Similarly to equation (2.10), the variances of the nth diagonal elements can be written as

$$\sigma_{dn}^2 = \frac{\tau_{dp} p_{dp} \zeta_{dn}^2}{1 + \tau_{dp} p_{dp} \zeta_{dn}}, \quad \text{and} \quad \xi_{dn}^2 = \frac{\zeta_{dn}}{1 + \tau_{dp} p_{dp} \zeta_{dn}}. \tag{2.12}$$

Here, p_{dp} is the transmit power of each pilot symbols and τ_{dp} is the number of pilot symbols transmitted from the relay station.

2.4 Decode-and-Forward Relay Signal Processing

In this section, a general signal model for multi-user massive MIMO relay networks operating over fading channels is presented. The schematic diagram of the multi-user relay network depicted in Figure 2.1 is used here for developing the corresponding signal model from the users to the destination. Here, N spatially distributed user nodes transmit their information via an intermediate relay. The processing matrices at the relay are denoted by $\mathbf{F}_s$ and $\mathbf{F}_d$, respectively.

2.4.1 Source to Relay Phase

Suppose the user nodes generate their original signal vectors $\mathbf{s} = [s_1, \cdots, s_N]^T$ meeting $E[\mathbf{s}\mathbf{s}^H] = \mathbf{I}_N$, where s_n is the symbol transmitted from the nth source UE to the relay. In S-R phase, the N source UEs simultaneously transmit their $N \times 1$ signal $\mathbf{x}_s = \sqrt{\mathbf{P}_s}\mathbf{s}$ to the relay where $\mathbf{P}_s = diag(p_{s1}, \cdots, p_{sN})$ is the power allocation matrix applied to all N source UEs. At this point, the signal vector $M \times 1$ received at the relay can be written as

$$\mathbf{y}_r = \mathbf{H}_s\mathbf{x}_s + \mathbf{w}_r, \tag{2.13}$$

where $\mathbf{H}_s$ is the channel matrix between the user nodes and relay, and $\mathbf{w}_r$ is an $M \times 1$ AWGN vector with zero-mean and unit variance. Next, the relay processes its received signal by using the $M \times N$ receive beamforming matrix $\mathbf{F}_s$. The received signal at the relay after applying the signal processing matrix F_s can thus be expressed as

$$\hat{\mathbf{y}}_r = \mathbf{F}_s^H\mathbf{y}_r = \mathbf{F}_s^H\mathbf{H}_s\mathbf{x}_s + \mathbf{F}_s^H\mathbf{w}_r. \tag{2.14}$$

Let $\hat{y}_{rn}$ denote the n-th component of the $N \times 1$ vector $\hat{\mathbf{y}}_r$. Then the received signal $\hat{y}_{rn}$ associated to the n-th user can be expressed as

$$\hat{y}_{rn} = \sqrt{p_{sn}}[\mathbf{f}_{sn}^H\mathbf{h}_{sn}]s_n + \sum_{i=1, i\neq n}^{N}\sqrt{p_{si}}[\mathbf{f}_{sn}^H\mathbf{h}_{si}]s_i + \mathbf{f}_{sn}^H\mathbf{w}_r, \tag{2.15}$$

$$= \sqrt{p_{sn}}[\mathbf{f}_{sn}^H\hat{\mathbf{h}}_{sn}]s_n + \sum_{i=1, i\neq n}^{N}\sqrt{p_{si}}[\mathbf{f}_{sn}^H\hat{\mathbf{h}}_{si}]s_i + \sum_{j=1}^{N}\sqrt{p_{sj}}[\mathbf{f}_{sn}^H\overline{\mathbf{h}}_{sj}]s_j + \mathbf{f}_{sn}^H\mathbf{w}_r, \tag{2.16}$$

where $\mathbf{f}_{sn}$ and $\hat{\mathbf{h}}_{sn}$ denote the nth column of matrix $\mathbf{F}_s$ and that of $\hat{\mathbf{H}}_s$, respectively. In (2.16), we see that the first term is the desired signal and the second term represents the interference. The third term can be considered as the additive noise caused by the channel estimation error and the fourth term is the white Gaussian noise independent of any transmit signal. Therefore, the received S-R SINR can be obtained as

$$\gamma_{sn} = \frac{p_{sn} \mid \mathbf{f}_{sn}^H \hat{\mathbf{h}}_{sn} \mid^2}{\sum\limits_{i=1, i\neq n}^{N} p_{si} \mid \mathbf{f}_{sn}^H \hat{\mathbf{h}}_{si} \mid^2 + \sum\limits_{j=1}^{N} p_{sj} \mid \mathbf{f}_{sn}^H \overline{\mathbf{h}}_{sj} \mid^2 + \parallel \mathbf{f}_{sn}^H \parallel^2}. \tag{2.17}$$

2.4.2 Relay to Destination Phase

During R-D phase, the relay simplifies the decoded information symbol vector $\hat{\mathbf{s}}$ of $\mathbf{s}$ from $\hat{\mathbf{y}}_r$ with $E[\hat{\mathbf{s}}\hat{\mathbf{s}}^H] = \mathbf{I}_N$, and multiplies it by the precoding matrix $\mathbf{F}_d$. The obtained signal vector after applying precoding matrix is $\mathbf{x}_r = \mathbf{F}_d\sqrt{\mathbf{P}_d}\hat{\mathbf{s}}$ and this signal is broadcast to all the N destination UEs. Here, $\mathbf{P}_d = diag(p_{d1}, \cdots, p_{dN})$ is the power allocation matrix used in the relay. Therefore, the relay forwards $\mathbf{x}_r$ signal to all the N destinations. The received $N \times 1$ signals $\mathbf{y}_d$ at the N destination UEs are given by

$$\mathbf{y}_d = \mathbf{H}_d^H \mathbf{x}_r + \mathbf{w}_d = \mathbf{H}_d^H \mathbf{F}_d \sqrt{\mathbf{P}_d}\hat{\mathbf{s}} + \mathbf{w}_d, \tag{2.18}$$

where $\mathbf{w}_d \in C^{N\times 1}$ denotes AWGN at the destination UEs which follows zero mean and unit variance. Therefore, the received signal at the nth destination UE is written as

$$y_{dn} = \sqrt{p_{dn}}[\mathbf{h}_{dn}^H \mathbf{f}_{dn}]\hat{s}_n + \sum_{i=1, i\neq n}^{N} \sqrt{p_{di}}[\mathbf{h}_{dn}^H \mathbf{f}_{di}]\hat{s}_i + w_{dn}.$$

$$= \sqrt{p_{dn}}[\hat{\mathbf{h}}_{dn}^H \mathbf{f}_{dn}]\hat{s}_n + \sum_{i=1, i\neq n}^{N} \sqrt{p_{di}}[\hat{\mathbf{h}}_{dn}^H \mathbf{f}_{di}]\hat{s}_i + \sum_{j=1}^{N} \sqrt{p_{dj}}[\overline{\mathbf{h}}_{dn}^H \mathbf{f}_{dj}]\overline{s}_j + w_{dn}. \tag{2.19}$$

where $\mathbf{f}_{dn}$ and $\hat{\mathbf{h}}_{dn}$ denote the nth column of matrix $\mathbf{F}_d$ and $\hat{\mathbf{H}}_d$, respectively, while w_{dn} is the nth element of $\mathbf{w}_d$. We assume, the precoding vector $\mathbf{f}_{dn}$ is normalized by $\mathbf{v}_d / \parallel \mathbf{v}_d \parallel$ at the relay station, then the received signal at the nth user can be expressed as

$$\hat{y}_{dn} = \sqrt{p_{dn}} \frac{\hat{\mathbf{h}}_{dn}^H \mathbf{v}_{dn}}{\parallel \mathbf{v}_{dn} \parallel} \hat{s}_n + \sum_{i=1, i\neq n}^{N} \sqrt{p_{di}} \frac{\hat{\mathbf{h}}_{dn}^H \mathbf{v}_{di}}{\parallel \mathbf{v}_{di} \parallel} \hat{s}_i + \sum_{j=1}^{N} \sqrt{p_{dj}} \frac{\overline{\mathbf{h}}_{dn}^H \mathbf{v}_{dj}}{\parallel \mathbf{v}_{dj} \parallel} \overline{s}_j + w_{dn} \tag{2.20}$$

Compared to the S-R transmission, only the first term in (2.20) is the desired signal, while the other three terms represent the interference, channel estimation error and white Gaussian noise,

respectively. From (2.20), the received SINR can be computed as

$$\gamma_{dn} = \frac{p_{dn} \frac{|\hat{\mathbf{h}}_{dn}^H \mathbf{v}_{dn}|^2}{\|\mathbf{v}_{dn}\|^2}}{\sum\limits_{i=1, i\neq n}^{N} p_{di} \frac{|\hat{\mathbf{h}}_{dn}^H \mathbf{v}_{di}|^2}{\|\mathbf{v}_{di}\|^2} + \sum\limits_{j=1}^{N} p_{dj} \frac{|\bar{\mathbf{h}}_{dn}^H \mathbf{v}_{dj}|^2}{\|\mathbf{v}_{dj}\|^2} + 1} \tag{2.21}$$

2.4.3 Linear Processing Schemes

This subsection gives a brief reviews of the signal processing aspects by applying linear processing schemes. The matrices $\mathbf{F}_s$ and $\mathbf{F}_d$ need to be designed to optimize the fundamental trade-off between the achievable performance and implementation complexity. Linear processing techniques have received wide attention for low implementation complexity and satisfactory performance. Due to the spectrum scarcity, wireless systems are likely to adopt aggressive frequency reuse policies in order to meet the increasing demand for high-quality wireless services. However, the use of the same frequency in the same cell site inevitably results in an interference-limited communication environment. When relaying technology is adopted in cellular systems, the co-channel interference environment becomes increasingly complex [54]. It is well known that massive MIMO technology provides extra spatial degrees of freedom, which can be efficiently utilized for CCI cancellation [12], [22]. The transmit antenna selection or maximum ratio combining (MRC) can improve the performance of massive MIMO operation. The main motivation for the use of linear combining schemes is to suppress the CCI and then forward the transformed signal to the destination by using the maximal ratio transmission (MRT).

In this context, MRC/MRT configurations are presented for the multi-user massive MIMO relay network shown in 2.1. For the MRC scheme, the receiver simply applies the principle of matched filtering to maximize the strength of the desired signal, ignoring the effect of interference. MRC is a method of diversity combining in which the signals from different channels are added together. The detection matrix is simply given by $\mathbf{F}_s = \hat{\mathbf{H}}_s$ where $\mathbf{f}_{sn}^H = \hat{\mathbf{h}}_{sn}^H$ for the nth user. From (2.17), the received SINR of nth user can be obtained as

$$\gamma_{sn} = \frac{p_{sn} \mid \hat{\mathbf{h}}_{sn}^H \hat{\mathbf{h}}_{sn} \mid^2}{\sum\limits_{i=1, i\neq n}^{N} p_{si} \mid \hat{\mathbf{h}}_{sn}^H \hat{\mathbf{h}}_{si} \mid^2 + \sum\limits_{j=1}^{N} p_{sj} \mid \hat{\mathbf{h}}_{sn}^H \bar{\mathbf{h}}_{sj} \mid^2 + \parallel \hat{\mathbf{h}}_{sn}^H \parallel^2},$$

$$= \frac{p_{sn} \parallel \hat{\mathbf{h}}_{sn} \parallel^4}{\sum\limits_{i=1, i\neq n}^{N} p_{si} \mid \hat{\mathbf{h}}_{sn}^H \hat{\mathbf{h}}_{si} \mid^2 + \sum\limits_{j=1}^{N} p_{sj} \mid \hat{\mathbf{h}}_{sn}^H \overline{\mathbf{h}}_{sj} \mid^2 + \parallel \hat{\mathbf{h}}_{sn}^H \parallel^2}. \tag{2.22}$$

After a successful detection, the relay employs MRT precoder for signal transmission to the destination. Precoding is a technique exploiting transmit diversity by weighting the information stream. MRT only maximizes the signal amplification at the intended user and it is close to optimal in noise-limited systems, where the inter-user interference is negligible compared to the noise. When MRT precoder is employed at relay system with precoding matrix $\mathbf{V} = \hat{\mathbf{H}}$, the received SINR can be written from equation (2.21) as

$$\gamma_{dn} = \frac{p_{dn} \frac{|\hat{\mathbf{h}}_{dn}^H \hat{\mathbf{h}}_{dn}|^2}{\|\hat{\mathbf{h}}_{dn}\|^2}}{\sum\limits_{i=1, i\neq n}^{N} p_{di} \frac{|\hat{\mathbf{h}}_{dn}^H \hat{\mathbf{h}}_{di}|^2}{\|\hat{\mathbf{h}}_{di}\|^2} + \sum\limits_{j=1}^{N} p_{dj} \frac{|\overline{\mathbf{h}}_{dn}^H \hat{\mathbf{h}}_{dj}|^2}{\|\hat{\mathbf{h}}_{dj}\|^2} + 1}, \tag{2.23}$$

$$= \frac{p_{dn} \| \hat{\mathbf{h}}_{dn} \|^2}{\sum\limits_{i=1, i\neq n}^{N} p_{di} \frac{|\hat{\mathbf{h}}_{dn}^H \hat{\mathbf{h}}_{di}|^2}{\|\hat{\mathbf{h}}_{di}\|^2} + \sum\limits_{j=1}^{N} p_{dj} \frac{|\overline{\mathbf{h}}_{dn}^H \hat{\mathbf{h}}_{dj}|^2}{\|\hat{\mathbf{h}}_{dj}\|^2} + 1}. \tag{2.24}$$

2.5 Energy Efficiency Metrics

EE is a well-known metric to demonstrate the performance of the 5G communication system. A lot of research and development efforts have been made in the wireless industry, aiming for effective solutions for energy efficient wireless communications. Since EE metric is the indicator of efficiency, it provides a better view of how EE can be achieved in wireless systems/networks by observing energy at every aspect of a wireless system and network. In this section, EE maximization is studied for wireless network level solution.

The EE of a communication system is measured in bit/Joule [20] which is estimated as the proportion between the channel capacity or average sum-rate (in bit/second) and the average total power consumption (in Watt = Joule/second). From wireless communications perspective, the cost is represented by the amount of energy consumed to operate the whole transceiver chain.

The sum-rate is another fundamental metric used for characterizing the achievable performance of multi-user wireless networks. It is the tight upper bound on the rate at which data can be reliably

sent over a communication channel. For the noisy-channel coding theorem, the capacity of a given channel is the highest information rate in units of data per unit time that can be achieved with arbitrarily small error probability. The channel capacity formula developed by Shannon provides a mathematical model of maximum mutual information between the input and output of the channel. The notion of channel capacity is fundamental to the evolution of advanced wireless communication systems. In section 2.4, we already discussed the SINR for MRC/MRT linear processing. Based on those SINR expressions, we can find the sum-rates for S-R and R-D channels as follows:

$$R_{MRC} = \frac{1}{2}\sum_{n=1}^{N} log_2(1+\gamma_{sn}), \tag{2.25}$$

$$R_{MRT} = \frac{1}{2}\sum_{n=1}^{N} log_2(1+\gamma_{dn}). \tag{2.26}$$

The above metrics provide quantified information to assess the efficiency of communication. EE metrics are usually employed for three purposes as

- First, to compare energy consumption performance of different components.
- Second, to set explicit long-term research and development targets on EE.
- Third, to reflect EE of certain configuration in a network and enable adjustment for more energy efficient configuration.

In a multi-user setting, the total EE metrics accounting for both S-R and R-D take the accompanying form,

$$EE_{MRC} = \frac{R_{MRC}}{P_{st}} = \frac{\frac{1}{2}\sum\limits_{n=1}^{N} log_2(1+\gamma_{sn})}{P_{st}}, \tag{2.27}$$

$$EE_{MRT} = \frac{R_{MRT}}{P_{dt}} = \frac{\frac{1}{2}\sum\limits_{n=1}^{N} log_2(1+\gamma_{dn})}{P_{dt}}. \tag{2.28}$$

where P_{st} is the total data transmission power from source to relay station and P_{dt} indicate the total power from relay to destination transmission, respectively.

2.6 Summary

At the beginning of this chapter, we presented a brief introduction about massive MIMO aided relay communication needed to develop the work in later chapters of this thesis. Then, we have discussed channel estimation by applying MMSE technique. The related signal processing tasks are briefly investigated in each transmission phase by using MRC/MRT linear processing techniques. We have derived an exact closed-form expression of EE of the underlying complex system for each transmission phase. As the main goal of this thesis is to investigate optimal power allocation for EE maximization, a non-convex power allocation optimization problem with the objective of EE maximization will be formulated under specific QoS and transmit power constraints in the next chapter. The closed form EE expressions will be utilized as the objective function in the desired optimization problem.

Chapter 3

Energy Efficiency Maximization for MIMO DF Relay

We have briefly introduced the massive MIMO DF-relay system in the previous chapter, where the source signal is processed at the relay by using MRC/MRT transceiver and the EE metrices are discussed based on sum-rates and overall transmit power. As shown, the EE can be improved by increasing SE and meanwhile decreasing the overall power consumption. Therefore, a non-convex power allocation optimization problem with the objective of maximizing the EE will be formulated in this chapter subject to the specific QoS and transmit power constraints for each transmission phase. Due to the non-convex characteristics of the problem, a successive convex optimization technique will be used to solve the problem based on some numerical optimization methods. Matlab simulations show the performance of EE improvement at the end of this chapter.

3.1 Mathematical Background

An optimization problem is finding the best solution from all feasible solutions. Since the late 1940s, a large effort has been done to develop algorithms for solving various classes of optimization problems, analyzing their properties, and developing efficient software packages [56]. In the last two decades, a large number of fundamental and practical results have been obtained in convex optimization theory [56], [57]. This is now a well-developed area, both in the theoretical and

practical aspects in the present scenario. The effectiveness of these algorithms depends on the particular forms of the objective and constraint functions. The objective function is often maximized or minimized subject to the constraints that may determine the choice of decision variable values. The general optimization problem is unpredictably hard to solve even when the objective and constraint functions are smooth. Nevertheless, there are some important exceptions to the general rule that make most optimization problems hard to resolve. For a few problem classes, we have effective algorithms that can reliably solve even large problems such as convex optimization [57].

Convex optimization methods have been used extensively in modeling, analyzing, and designing communication systems [57], [58]. In particular, the popularity of convex optimization is due to the fact that many problems in communications and signal processing can be naturally formulated or recast as convex optimization problems. Theoretically, convex optimization is appealing since a local optimum is also a global optimum and the computation effort required to find the global optimum is much less as compared to the problems with multiple local optimums. Convex optimization is also attractive because it usually reveals insight into the structure of the optimal solution and the design itself. Furthermore, the availability of software like CVX [49], for solving convex problems make convex optimization even more popular. Suppose, S is a subset of $\mathbf{R}^n$ for $n \geq 1$. A function $f : \mathbf{R}^n \rightarrow \mathbf{R}$ on a convex set S^1 is a convex function if, for any two points $x, y \in S$, it satisfies

$$f(\theta x + (1-\theta)y) \leq \theta f(x) + (1-\theta)f(y). \quad 0 \leq \theta \leq 1 \tag{3.1}$$

In other words, along any line segment in S, $f(\theta x + (1-\theta)y)$ is the weighted average for x and y which is less than or equal to the individual weighted average of $f(x)$ and $f(y)$. One says f is concave if $(-f)$ is convex. Convex functions are closed under summation, positive scaling, and point wise maximum operation. More detailed description of convex set and convex function is provided in Appendix A.

3.1.1 Convex Optimization in Standard Form

A convex optimization problem with arbitrary equality and inequality constraints can always be written in the following standard forms [57].

$$\min_{x} f_0(x), \tag{3.2a}$$

$$s.t., \quad f_i(x) \leq 0, \quad i = [1, \cdots, p], \tag{3.2b}$$

$$h_i(x) = 0, \quad i = [1, \cdots, q], \tag{3.2c}$$

$$x \in S, \tag{3.2d}$$

where f_0 is the objective function; $f_i(x)$, and $h_i(x)$ are the inequality and equality constraint functions, respectively, and S is the constraint set. The optimization problem in (3.2) is a convex optimization problem if the objective and inequality constraint functions are convex and the equality constraint functions are linear. The equality constraints $h_i(x) = 0$, $i = 1, \cdots, q$ can be represented by matrix equation $\mathbf{Ax} = \mathbf{b}$, where $\mathbf{A}$ and $\mathbf{b}$ are matrix and vector of appropriate sizes. The optimization variable x is said to be feasible if $x \in S$ and it satisfies all the inequality and equality constraints. A feasible solution x^* is said to be globally optimal if for all feasible solution x, $f_0(x^*) \leq f_0(x)$.

In communication systems, when a power allocation problem is addressed, it often happens that the objective(s) and constraint sets are non-convex, which makes the problem hard to solve, so even mentioning the global optimum. Fortunately, many of such optimization problems have hidden convexity and can be equivalently recast as convex problems. Generally speaking, the non-convex problem can be reformulated in convex form by using a series of clever transforms of variables. Nevertheless, it is not always possible to devise a convex problem that is exactly equivalent to the original one. In fact, it would suffice if they both have the same set of optimal solutions. In other words, both the original non-convex and the reformulated convex problems have to be equivalent only within the set of optimal solutions.

During the last decade, there has been a tremendous endeavor in developing efficient algorithms for solving a wide range of convex optimization problems [57]. A remarkable example of this approach is the family of geometric programming (GP) [48], [56]. This is a really interesting and useful class of problems which are not convex in their natural form but can be transformed into a convex problem. GP is now well-known for modeling, and analyzing the communication systems.

3.1.2 Geometric Programming

GP is a class of optimization problem with many useful theoretical and computational properties [56]. GP substantially broadens the scope of convex applications and is naturally suited to model various types of important non-linear systems in science and engineering. Since its inception in 1960s, GP has found applications in mechanical and civil engineering, chemical engineering, probability and statistics, finance and economics, control theory, etc. [56]. In recent years, GP has been widely utilized to study a variety of problems in the analysis and invention of communication systems, information and queuing theory, coding and signal processing, wireless networking and network protocols [46], [48].

GP is a branch of nonlinear programming dealing with the problem of minimizing a monomial or posynomial subject to certain posynomial inequality constraints. Let $x_1, \cdots, x_k$ denote k real positive variables components of x. A real valued function f of x in the following form

$$f(x) = cx_1^{a_1} x_2^{a_2} \cdots x_k^{a_k}, \tag{3.3}$$

where $c > 0$ and $a_j \in \mathbf{R}$, $j = 1, \cdots, k$, is called a monomial of the variables $x_1, \cdots, x_k$. The constant c is the coefficient of the monomial, and $a_1, \cdots, a_k$ is the exponents of the monomial. A posynimial function is the sum of one or more monomials, i.e., a function of the form

$$f(x) = \sum_{n=1}^{N} c_n x_1^{a_{1n}} x_2^{a_{2n}} \cdots x_k^{a_{kn}}, \tag{3.4}$$

where $c_n > 0$ is called a posynomial function with N terms of the variables $x_1, \cdots, x_k$. A GP problem in its standard form can be written as follows [48],

$$\min_x f_0(x), \tag{3.5a}$$

$$s.t. \quad f_i(x) \leq 0, \quad i = [1, \cdots, p], \tag{3.5b}$$

$$h_i(x) = 0, \quad i = [1, \cdots, q], \tag{3.5c}$$

where f_i, $i = 1, \cdots, p$ are posynomials and h_i, $i = 1, \cdots, q$ are monomials, i.e., inequality constraint functions are posynomials and equality constraint functions are monomials. The standard form of GP is non-linear. However, a logarithmic change of the variables, multiplicative constants, and the function values may build an equivalent convex problem in the form of new variables. On the other hand, a serious restriction in the diligence of the theory of GP to real engineering problems has been that the theory can deal exclusively with positive conditions. Therefore, GP has been be extended to complementary geometric programming (CGP) to include any rational function of posynomial terms.

A program formulated in terms of a rational function of posynomial terms called CGP [46]. While GP has the remarkable property that every constrained local minimum is also a global minimum, no such claim can generally be made for CGP, since CGP is the extended version of the theory of GP including any rational function of posynomial term. The algorithm CGP is derived for successively approximating rational function of posynomial terms by posynomials which involves solving a sequence of GP. In the next section, we are going to introduce an EE optimization problem which will then be reformulated later via CGP and GP.

3.2 Proposed Optimization Problem

3.2.1 Energy Efficiency Maximization

In this section, we present an optimization problem to maximize the EE subject to the total transmit power and individual user and pilot powers for the S-R and R-D phases. We focus on the S-R phase since the R-D phase is very similar. Using (2.27), the optimal EE for S-R under MRC can be described as

$$EE_{MRC}^{max} = \max_{p_{sp}, p_{sn}} \frac{R_{MRC}}{P_{st}} = \max_{p_{sp}, p_{sn}} \frac{1}{2P_{st}} \sum_{n=1}^{N} log_2(1 + \gamma_{sn}), \tag{3.6a}$$

$$s.t. \quad \tau_{sn} p_{sn} + \tau_{sp} p_{sp} \leq P_{st}, \tag{3.6b}$$

$$0 \leq p_{sn} \leq P_s^{max}, \quad 0 \leq p_{sp} \leq P_p^{max}, \tag{3.6c}$$

where P_s^{max} and P_p^{max} are the maximum power limits for each user and pilot, respectively. Obviously, the objective function $(3.6a)$ can be modified and rewritten as

$$EE_{MRC}^{max} = \max_{p_{sp},p_{sn}} \frac{1}{2P_{st}} log_2 \prod_{n=1}^{N}(1+\gamma_{sn}). \tag{3.7}$$

Since $log_2(x)$ is an increasing function of x, the objective function in (3.7) can be equivalently rewritten as

$$EE_{MRC}^{max} = \frac{1}{2P_{st}} \min_{p_{sp},p_{sn}} \prod_{n=1}^{N} \frac{1}{(1+\gamma_{sn})} \tag{3.8}$$

where $\frac{1}{2}$ is a multiplicative constant and it does not affect the problem solution. Here, P_{st} is measured from uniform power allocation. Therefore, (3.6) can be rewritten as

$$\min_{p_{sp},p_{sn}} \prod_{n=1}^{N} \frac{1}{(1+\gamma_{sn})}, \tag{3.9a}$$

$$s.t. \quad \tau_{sn}p_{sn} + \tau_{sp}p_{sp} \leq P_{st}, \tag{3.9b}$$

$$0 \leq p_{sn} \leq P_s^{max}, \quad 0 \leq p_{sp} \leq P_p^{max}. \tag{3.9c}$$

Here, (3.9) is an optimization problem subject to the inequality constraint functions. The optimization variables p_{sp} and p_{sn} are said to be feasible if they satisfy all the inequality constraints. Let p_{sp}^* and p_{sn}^* be globally optimal solutions that are feasible solutions of γ_{sn}^* and satisfy $p_{sp}^* \leq p_{sp}$ and $p_{sn}^* \leq p_{sn}$, respectively. Apparently, the constraints in (3.9) are convex functions but the objective is non-convex rational function. A rational objective function is very difficult to solve. Therefore, we reformulate the objective function into a convex function using CGP to solve it via simple CVX toolbox [49].

3.2.2 Problem Reformulation

In this subsection, we reformulate the objective function to obtain a modified problem for power allocation optimization problem (3.9). Using standard reformulation technique, the objective function is converted to an equivalent CGP [46] in order to obtain a successive approximation optimization problem for this DF-relay system. Mainly, we solve the objective function for MRC S-R, which

will be followed by the same concept for the MRT transmission in the R-D link. By definition, the CGP is approximated as the rational function of posynomial terms by posynomials. Therefore, the approximation for the objective term (3.9) can be described by the following lemma [45]

Lemma: For any $\gamma > 0$, let $E(\gamma) = \lambda\gamma^{\delta}$ be a monomial function that is used to approximate $F(\gamma) = 1 + \gamma$ near an arbitrary point $\hat{\gamma} > 0$. Then, the following two conditions are held.

- The parameters δ and λ of the best monomial local approximation are given by

$$\delta = \hat{\gamma}(1 + \hat{\gamma})^{-1}, \quad \lambda = \hat{\gamma}^{-\delta}(1 + \hat{\gamma}). \tag{3.10}$$

- $F(\gamma) \geq E(\gamma)$ for all $\gamma > 0$.

By replacing the expressions of E and F, we obtain $1+\gamma \geq \lambda\gamma^{\delta}$. Therefore, using the monomial approximation given by lemma, the rational objective function $(1+\gamma_{sn})^{-1}$ of (3.9) is approximated $\lambda_{sn}^{-1}{\gamma_{sn}}^{-\delta_{sn}}$ near the point $\hat{\gamma}_{sn}$ where, δ_{sn} and λ_{sn} can be written using (3.10) as

$$\delta_{sn} = \hat{\gamma}_{sn}(1 + \hat{\gamma}_{sn})^{-1}, \quad \lambda_{sn} = \hat{\gamma}_{sn}^{-\delta_{sn}}(1 + \hat{\gamma}_{sn}). \tag{3.11}$$

Consequently, the approximated objective function can be written as

$$(1 + \gamma_{sn})^{-1} \geq \lambda_{sn}^{-1}{\gamma_{sn}}^{-\delta_{sn}}. \tag{3.12}$$

As the objective function of (3.12) is a decreasing function of $(1 + \gamma_{sn})^{-1}$, it can easily be verified that the modified objective function will be usable in the solution of the GP. GP can be reformulated as convex problems, and it can very efficiently be solved even for large-scale problems [48]. By starting from an initial point, we can search for a close local optimum by solving a sequence of GPs that locally approximate the original problem (3.9). At each step, the GP is obtained by replacing the rational objective function with their best local monomial approximation near the solution obtained at the previous step. Therefore, we can use the SINR expressions from (2.22) and (2.24) as a constraint function to optimize γ_{sn} and γ_{dn} variables. Including (2.22) and (2.24) as constraint function, we can established two different optimization problems for S-R and R-D from

(3.9). In the S-R phase, we have

$$\min_{p_{sp},p_{sn},\gamma_{sn}} \prod_{n=1}^{N} \lambda_{sn}^{-1} {\gamma_{sn}}^{-\delta_{sn}}, \tag{3.13a}$$

$$s.t. \quad \gamma_{sn} = \frac{p_{sn} \parallel \hat{\mathbf{h}}_{sn} \parallel^4}{\sum\limits_{i=1,i\neq n}^{N} p_{si} \mid \hat{\mathbf{h}}_{sn}^H \hat{\mathbf{h}}_{si} \mid^2 + \sum\limits_{j=1}^{N} p_{sj} \mid \hat{\mathbf{h}}_{sn}^H \overline{\mathbf{h}}_{sj} \mid^2 + \parallel \hat{\mathbf{h}}_{sn}^H \parallel^2}, \tag{3.13b}$$

$$\tau_{sn} p_{sn} + \tau_{sp} p_{sp} \leq P_{st}, \tag{3.13c}$$

$$0 \leq p_{sn} \leq P_s^{max}, \quad 0 \leq p_{sp} \leq P_p^{max}. \tag{3.13d}$$

In the case of the R-D phase, the optimization problem can be modified as

$$\min_{p_{dp},p_{dn},\gamma_{dn}} \prod_{n=1}^{N} \lambda_{dn}^{-1} {\gamma_{dn}}^{-\delta_{dn}}, \tag{3.14a}$$

$$\gamma_{dn} = \frac{p_{dn} \parallel \hat{\mathbf{h}}_{dn} \parallel^2}{\sum\limits_{i=1,i\neq n}^{N} p_{di} \frac{|\hat{\mathbf{h}}_{dn}^H \hat{\mathbf{h}}_{di}|^2}{\|\hat{\mathbf{h}}_{di}\|^2} + \sum\limits_{j=1}^{N} p_{dj} \frac{|\bar{\mathbf{h}}_{dn}^H \hat{\mathbf{h}}_{dj}|^2}{\|\hat{\mathbf{h}}_{dj}\|^2} + 1}, \tag{3.14b}$$

$$\tau_{dn} p_{dn} + \tau_{dp} p_{dp} \leq P_{dt}, \tag{3.14c}$$

$$0 \leq p_{dn} \leq P_d^{max}, \quad 0 \leq p_{dp} \leq P_p^{max}, \tag{3.14d}$$

where p_{dn} and p_{dp} are the individual user and pilot power respectively, and P_{dt} is the total power for R-D transmission. Observing (3.13) and (3.14), the objective functions are now a monomial function. However, this is another new challenge appeared because the right-hand sides (RHS) of the constraint functions are neither monomial nor posynomial. To solve this non-convex rational function, we are going to introduce a lower bound of the average SINR for our proposed DF-relay system [21], [47] and use them in (3.13) and (3.14) to replace the real SINR.

3.3 Lower Bound Average SINR

A lower bound of the average SINR has been derived by discovering the relationship between the overall transmit power and average SINR [47]. Here, we need to consider the conventional linear

MRC/MRT processing for the S-R and R-D transmission, respectively. The statistical SINR for S-R and R-D are already defined in (2.22) and (2.24). Therefore, dividing the (2.22) by $\parallel \hat{\mathbf{h}}_{sn} \parallel^2$, we get the SINR for MRC as given by

$$\gamma_{sn} = \frac{p_{sn} \parallel \hat{\mathbf{h}}_{sn} \parallel^2}{\sum\limits_{i=1, i\neq n}^{N} p_{si} \frac{|\hat{\mathbf{h}}_{sn}^H \hat{\mathbf{h}}_{si}|^2}{\|\hat{\mathbf{h}}_{sn}\|^2} + \sum\limits_{j=1}^{N} p_{sj} \frac{|\hat{\mathbf{h}}_{sn}^H \overline{\mathbf{h}}_{sj}|^2}{\|\hat{\mathbf{h}}_{sn}\|^2} + 1}. \tag{3.15}$$

Averaging both sides of (3.15), the S-R average SINR can be expressed as

$$E\left[\gamma_{sn}\right] = E\left[\frac{p_{sn} \parallel \hat{\mathbf{h}}_{sn} \parallel^2}{\sum\limits_{i=1, i\neq n}^{N} p_{si} \frac{|\hat{\mathbf{h}}_{sn}^H \hat{\mathbf{h}}_{si}|^2}{\|\hat{\mathbf{h}}_{sn}\|^2} + \sum\limits_{j=1}^{N} p_{sj} \frac{|\hat{\mathbf{h}}_{sn}^H \overline{\mathbf{h}}_{sj}|^2}{\|\hat{\mathbf{h}}_{sn}\|^2} + 1}\right], \tag{3.16}$$

where the elements of $\hat{\mathbf{h}}_{si}$ and $\overline{\mathbf{h}}_{sj}$ vectors consist of i.i.d. zero-mean Gaussian RVs [21], [60, chapter 4]. Therefore, both $\frac{\hat{\mathbf{h}}_{sn}^H \hat{\mathbf{h}}_{si}}{\|\hat{\mathbf{h}}_{sn}\|}$ and $\frac{\hat{\mathbf{h}}_{sn}^H \overline{\mathbf{h}}_{sj}}{\|\hat{\mathbf{h}}_{sn}\|}$ are Gaussian random variables conditioned on $\hat{\mathbf{h}}_{sn}$ but do not depend on $\hat{\mathbf{h}}_{sn}$ [21]. Accordingly, the numerator is independent of the three terms in the denominator (3.16). Thus, we have

$$E\left[\gamma_{sn}\right] = E[\parallel \hat{\mathbf{h}}_{sn} \parallel^2] \frac{p_{sn}}{E\left[\sum\limits_{i=1, i\neq n}^{N} p_{si} \frac{|\hat{\mathbf{h}}_{sn}^H \hat{\mathbf{h}}_{si}|^2}{\|\hat{\mathbf{h}}_{sn}\|^2} + \sum\limits_{j=1}^{N} p_{sj} \frac{|\hat{\mathbf{h}}_{sn}^H \overline{\mathbf{h}}_{sj}|^2}{\|\hat{\mathbf{h}}_{sn}\|^2} + 1\right]}. \tag{3.17}$$

Nothing the fact that the function $1/x$ is convex when x is positive and using the Jensens inequality (see Appendix B.2 for the details of Jensens inequality), (3.17) can be further expressed as

$$E\left[\gamma_{sn}\right] \geq E[\parallel \hat{\mathbf{h}}_{sn} \parallel^2] \frac{p_{sn}}{\sum\limits_{i=1, i\neq n}^{N} p_{si} E[\frac{|\hat{\mathbf{h}}_{sn}^H \hat{\mathbf{h}}_{si}|^2}{\|\hat{\mathbf{h}}_{sn}\|^2}] + \sum\limits_{j=1}^{N} p_{sj} E[\frac{|\hat{\mathbf{h}}_{sn}^H \overline{\mathbf{h}}_{sj}|^2}{\|\hat{\mathbf{h}}_{sn}\|^2}] + 1}. \tag{3.18}$$

From the property of spherically symmetric distribution [21], [60, chapter 4], $\frac{\hat{\mathbf{h}}_{sn}^H \hat{\mathbf{h}}_{si}}{\|\hat{\mathbf{h}}_{sn}\|}$ and $\frac{\hat{\mathbf{h}}_{sn}^H \overline{\mathbf{h}}_{sj}}{\|\hat{\mathbf{h}}_{sn}\|}$ are Gaussian RVs with zero mean and variance σ_{si}^2 and ξ_{sj}^2, respectively. Therefore, (3.18) can be simplified as

$$E\left[\gamma_{sn}\right] \geq E[\parallel \hat{\mathbf{h}}_{sn} \parallel^2] \frac{p_{sn}}{\sum\limits_{i=1,i\neq n}^{N} p_{si}\sigma_{si}^2 + \sum\limits_{j=1}^{N} p_{sj}\xi_{sj}^2 + 1}. \tag{3.19}$$

From the MMSE channel estimation in section 2.3.2, we can see that $\hat{\mathbf{H}}_s$ is independent of $\overline{\mathbf{H}}_s$. The elements of vector $\hat{\mathbf{h}}_{sn}$ are i.i.d. Gaussian variables with zero mean and constant variance $\frac{\zeta_{sn}^2 \tau_{sp} p_{sp}}{1+\zeta_{sn}\tau_{sp}p_{sp}}$. Therefore, the term $\parallel \hat{\mathbf{h}}_{sn} \parallel^2$ in (3.19) can be treated as a 1×1 central complex Wishart matrix with M degrees of freedom [61]. The detailed properties of central Wishart matrix are given in Appendix B.3. From the property of central Wishart matrix equation $B.4$ [61], we have

$$E[\parallel \hat{\mathbf{h}}_{sn} \parallel^2] = E[\left(\hat{\mathbf{H}}_s^H \hat{\mathbf{H}}_s\right)_{nn}] = \frac{1}{N} E[tr\left(\hat{\mathbf{H}}_s^H \hat{\mathbf{H}}_s\right)] = \frac{M\zeta_{sn}^2 \tau_{sp} p_{sp}}{1+\zeta_{sn}\tau_{sp}p_{sp}}. \tag{3.20}$$

Substituting (3.19) and (3.20) into (3.18), we can get

$$E[\gamma_{sn}] \geq \frac{\frac{M\zeta_{sn}^2 \tau_{sp} p_{sp} p_{sn}}{1+\zeta_{sn}\tau_{sp}p_{sp}}}{\sum\limits_{i=1,i\neq n}^{N} \zeta_{si} p_{si} + p_{sn} \frac{\zeta_{sn}}{1+\zeta_{sn}\tau_{sp}p_{sp}} + 1}. \tag{3.21}$$

Here, (3.21) is the final lower bound of S-R average SINR of user n under MMSE channel estimation. The lower bound of average SINR for R-D phase can be calculated from the equation (2.24) when MRT transmitter is employed at the relay. Dividing the numerator and denominator of (2.24) by $\parallel \hat{\mathbf{h}}_{dn} \parallel^2$ leads to

$$\gamma_{dn} = \frac{p_{dn}}{\sum\limits_{i=1,i\neq n}^{N} p_{di} \frac{|\hat{\mathbf{h}}_{dn}^H \mathbf{h}_{di}|^2}{\|\mathbf{h}_{di}\|^2 \|\mathbf{h}_{dn}\|^2} + \sum\limits_{j=1}^{N} p_{dj} \frac{|\bar{\mathbf{h}}_{dn}^H \mathbf{h}_{dj}|^2}{\|\mathbf{h}_{dj}\|^2 \|\mathbf{h}_{dn}\|^2} + \frac{1}{\|\mathbf{h}_{dn}\|^2}}. \tag{3.22}$$

Averaging both sides of (3.22), we obtain

$$E\left[\gamma_{dn}\right] = \frac{p_{dn}}{E\left[\sum\limits_{i=1,i\neq n}^{N} p_{di} \frac{|\hat{\mathbf{h}}_{dn}^H \mathbf{h}_{di}|^2}{\|\mathbf{h}_{di}\|^2 \|\mathbf{h}_{dn}\|^2} + \sum\limits_{j=1}^{N} p_{dj} \frac{|\bar{\mathbf{h}}_{dn}^H \mathbf{h}_{dj}|^2}{\|\mathbf{h}_{dj}\|^2 \|\mathbf{h}_{dn}\|^2} + \frac{1}{\|\mathbf{h}_{dn}\|^2}\right]}. \tag{3.23}$$

Applying Jensens inequality in (3.23), the average SINR satisfies

$$E\left[\gamma_{dn}\right] \geq \frac{p_{dn}}{\sum\limits_{i=1,i\neq n}^{N} p_{di} E\left[\mid \frac{\hat{\mathbf{h}}_{dn}^{H}\mathbf{h}_{di}}{\|\mathbf{h}_{di}\|\|\hat{\mathbf{h}}_{dn}\|} \mid^{2}\right] + E\left[\frac{1}{\|\mathbf{h}_{dn}\|^{2}}\right] \sum\limits_{j=1}^{N} p_{dj} E\left[\frac{|\bar{\mathbf{h}}_{dn}^{H}\mathbf{h}_{dj}|^{2}}{\|\mathbf{h}_{dj}\|^{2}}\right] + E\left[\frac{1}{\|\mathbf{h}_{dn}\|^{2}}\right]}. \quad (3.24)$$

Observing (3.24), $\frac{\bar{\mathbf{h}}_{dn}^{H}\mathbf{h}_{dj}}{\|\mathbf{h}_{dj}\|^{2}}$ is a Gaussian random variable with zero mean and variance ξ_{dj}^{2}. The vector $\frac{\hat{\mathbf{h}}_{dn}}{\|\hat{\mathbf{h}}_{dn}\|}$ is spherically symmetric [60, chapter 4]. Therefore, the elements of $\frac{\hat{\mathbf{h}}_{dn}}{\|\hat{\mathbf{h}}_{dn}\|}$ are uncorrelated and independent RVs following a unit spherical distribution with zero mean and variance $(1/M)$. Moreover, the two vectors $\frac{\hat{\mathbf{h}}_{dn}}{\|\hat{\mathbf{h}}_{dn}\|}$ and $\hat{\mathbf{h}}_{di}$ are independent when $i \neq n$. From the property of spherical distribution, $\frac{\hat{\mathbf{h}}_{dn}^{H}}{\|\hat{\mathbf{h}}_{dn}\|}$ $\frac{\hat{\mathbf{h}}_{di}}{\|\hat{\mathbf{h}}_{di}\|}$ follows a unit spherical distribution with zero mean and variance $1/M$. Therefore, we have $E[\mid \frac{\hat{\mathbf{h}}_{dn}^{H}}{\|\hat{\mathbf{h}}_{dn}\|}\frac{\hat{\mathbf{h}}_{di}}{\|\hat{\mathbf{h}}_{di}\|} \mid^{2}] = \frac{1}{M}$. Further, from the property of central Wishart matrix [61] and very long random vectors [21], we get

$$E\left[\frac{1}{\| \hat{\mathbf{h}}_{dn} \|^{2}}\right] = E\left\{[\left(\hat{\mathbf{H}}_{s}^{H}\hat{\mathbf{H}}_{s}\right)^{-1}]_{nn}\right\} = \frac{1}{N}E[tr\left(\hat{\mathbf{H}}_{s}^{H}\hat{\mathbf{H}}_{s}\right)^{-1}] = \frac{1}{(M-1)\sigma_{dn}^{2}}. \quad (3.25)$$

Substituting (3.25) into (3.24), gives

$$E[\gamma_{dn}] \geq \frac{p_{dn}}{\frac{1}{M}\sum\limits_{i=1,i\neq n}^{N} p_{di} + \frac{1}{(M-1)\sigma_{dn}^{2}}\sum\limits_{j=1}^{N} p_{dj}\xi_{dj}^{2} + \frac{1}{(M-1)\sigma_{dn}^{2}}}. \quad (3.26)$$

Appling the value of σ_{dn}^{2} and ξ_{dn}^{2} from (2.12) to (3.26) and performing some manipulations, we get the final lower bound of the R-D average SINR under MMSE channel estimation,

$$E[\gamma_{dn}] \geq \frac{\frac{(M-1)\zeta_{dn}^{2}\tau_{dp}p_{dp}}{1+\zeta_{dn}\tau_{dp}p_{dp}}p_{dn}}{\frac{(M-1)\zeta_{dn}^{2}\tau_{dp}p_{dp}}{M(1+\zeta_{dn}\tau_{dp}p_{dp})}\sum\limits_{j=1,j\neq n}^{N} p_{di} + \sum\limits_{j=1}^{N} p_{dj}\frac{\zeta_{dn}}{1+\zeta_{dn}\tau_{dp}p_{dp}} + 1}. \quad (3.27)$$

3.4 Proposed Algorithms for Optimal Solution

This section demonstrates the final EE algorithm for massive MIMO DF-relay systems for each transmission phase. At the beginning, we use the lower bound of average SINR as a constraint function in (3.13) and (3.14) instead of the statistical SINR. Then, we modify the average SINR by

changing the variables to make standard GP format. Finally, we proceed to establish two algorithms for S-R and R-D transmission using two different optimization problems, respectively.

3.4.1 MRC: Source to Relay

We first rewrite the optimization problem (3.13) using the average SINR (3.21) as a constraint function, and let $\bar{\gamma}_{sn} = E[\gamma_{sn}]$ for notational simplicity. Thus, we have

$$\min_{p_{sp}, p_{sn}, \bar{\gamma}_{sn}} \prod_{n=1}^{N} \lambda_{sn}^{-1} \bar{\gamma}_{sn}^{-\delta_{sn}}, \tag{3.28a}$$

$$s.t. \quad \bar{\gamma}_{sn} \geq \frac{\frac{M\zeta_{sn}^2 \tau_{sp} p_{sp} p_{sn}}{1+\zeta_{sn}\tau_{sp}p_{sp}}}{\sum\limits_{i=1, i\neq n}^{N} \zeta_{si} p_{si} + p_{sn} \frac{\zeta_{sn}}{1+\zeta_{sn}\tau_{sp}p_{sp}} + 1}, \tag{3.28b}$$

$$\tau_{sn} p_{sn} + \tau_{sp} p_{sp} \leq P_{st}, \tag{3.28c}$$

$$0 \leq p_{sn} \leq P_s^{max}, \quad 0 \leq p_{sp} \leq P_p^{max}. \tag{3.28d}$$

It is easy to show that the optimization problem is still non-convex. To overcome this difficulty, we introduce a new set of variables in order to simplify the constraint functions in (3.28)

$$\alpha_{sn} = \frac{\zeta_{sn}}{1 + \zeta_{sn}\tau_{sp}p_{sp}}, \quad Or, \quad \tau_{sp}p_{sp} = \frac{1}{\alpha_{sn}} - \frac{1}{\zeta_{sn}}. \tag{3.29}$$

Since the range of p_{sp} is $(0, +\infty)$, we have $0 \leq \alpha_{sn} \leq \zeta_{sn}$ from (3.29). Substituting (3.29) into the constraint $(3.28b)$ and carrying out some manipulations, the first constraint function can be written as

$$\sum_{i=1, i\neq n}^{N} \zeta_{si} p_{si} p_{sn}^{-1} \bar{\gamma}_{sn} + p_{sn}^{-1} \bar{\gamma}_{sn} + M\alpha_{sn} + \alpha_{sn}\bar{\gamma}_{sn} \leq M\zeta_{sn}. \tag{3.30}$$

Substituting $\tau_{sp}p_{sp}$ from (3.29) into $(3.28c)$, we can rewrite the constraint function as

$$\alpha_{sn}^{-1} + p_{sn}\tau_{sn} \leq P_{st} + \zeta_{sn}^{-1}. \tag{3.31}$$

Finally, substituting (3.30) and (3.31) into (3.28), the optimal problem can be rewritten as

$$\min_{\alpha_{sn},p_{sn},\bar{\gamma}_{sn}} \prod_{n=1}^{N} \lambda_{sn}^{-1}\bar{\gamma}_{sn}^{-\delta_{sn}}, \tag{3.32a}$$

$$\sum_{i=1,i\neq n}^{N} \zeta_{si}p_{si}p_{sn}^{-1}\bar{\gamma}_{sn} + p_{sn}^{-1}\bar{\gamma}_{sn} + M\alpha_{sn} + \alpha_{sn}\bar{\gamma}_{sn} \leq M\zeta_{sn}, \tag{3.32b}$$

$$\alpha_{sn}^{-1} + \tau_{sn}p_{sn} \leq P_{st} + \zeta_{sn}^{-1}, \tag{3.32c}$$

$$0 \leq p_{sn} \leq P_{s}^{max}, \quad 0 \leq \alpha_{sn} \leq \zeta_{sn}. \tag{3.32d}$$

We substitute $0 \leq p_{sp} \leq P_{p}^{max}$ with $0 \leq \alpha_{sn} \leq \zeta_{sn}$ because p_{sp} is already changed by α_{sn} variable in (3.29). Now, the optimization problem in (3.32) is a standard GP problem [48]. It is known that such a GP problem can be solved by using some standard numerical optimization packages, for example, MOSEK [62], GPCVX [63] and ConVeX (CVX) [49]. Utilizing these standard packages, the obtained solution is recognized as globally optimal. It is worth remarking that all the variables in (3.32) are non-negative. The optimization problem can be changed over to a convex problem through a logarithmic transform of the variables. Based on this optimization problem, this thesis develops a computationally efficient algorithm to obtain the optimal solution based on the homotopy or continuation method. This algorithm is solved by an approximate version of (3.9) in every iteration. More detailed description of homotopy or continuation method is given in Appendix B.1. A brief synopsis of the proposed successive approximation algorithm is presented in Algorithm 1 to allocate all transmit powers of the S-R transmission phase. The algorithm has the following six steps to complete the iteration and reach the optimal solution

(1) The first step initializes the algorithm, and obtains a feasible SINR $\hat{\gamma}_{sn}$ from the initial power allocation. We set a parameter $\beta > 1$ to get the desired approximation accuracy of the SINR. A value of β close to 1 provides a good accuracy for the monomial approximations. At every step, each entry of the current SINR guess can be increased or decreased at most by a factor β. The maximum number of iterations is limit to $L = 15$ and a tolerance point is defined as $\varepsilon = 0.01$ as to compare between initial and optimal SINR values.

Algorithm 1 Successive approximation algorithm for S-R EE maximization

(1) **Initialization:** Given tolerance $\varepsilon > 0$, parameter $\beta = 1.1$ used to check the desired approximation accuracy, and the maximum number of iterations $L = 15$ with initial value $l = 1$. The initial value $\hat{\gamma}_{sn,l}$ for $(n = 1, 2, \cdots N)$ is obtained from the initial power allocation.

(2) **Computation:** Compute $\delta_{sn,l} = \hat{\gamma}_{sn,l}(1 + \hat{\gamma}_{sn,l})^{-1}, \quad \lambda_{sn,l} = \hat{\gamma}_{sn,l}^{-\delta_{sn,l}}(1 + \hat{\gamma}_{sn,l})$.

(3) **GP Optimization:**

$$\min_{\alpha_{sn}, p_{sn}, \bar{\gamma}_{sn}} \prod_{n=1}^{N} \lambda_{sn,l}^{-1} \bar{\gamma}_{sn}^{-\delta_{sn,l}},$$

$$\beta^{-1}\hat{\gamma}_{sn,l} \leq \bar{\gamma}_{sn} \leq \beta\hat{\gamma}_{sn,l},$$

$$\sum_{i=1, i\neq n}^{N} \zeta_{si} p_{si} p_{sn}^{-1} \bar{\gamma}_{sn} + p_{sn}^{-1}\bar{\gamma}_{sn} + M\alpha_{sn} + \alpha_{sn}\bar{\gamma}_{sn} \leq M\zeta_{sn},$$

$$\alpha_{sn}^{-1} + \tau_{sn} p_{sn} \leq P_{st} + \zeta_{sn}^{-1},$$

$$0 \leq p_{sn} \leq P_s^{max}, \quad 0 \leq \alpha_{sn} \leq \zeta_{sn}.$$

(4) **Stopping criterion:** If $\mid \bar{\gamma}_{sn}^{*} - \hat{\gamma}_{sn,l} \mid < \varepsilon$, stop the iteration; and directly go to step 6.

(5) **Setting:** Set $l = l + 1$, and update $\hat{\gamma}_{sn,l} = \bar{\gamma}_{sn}^{*}$. If $l < L = 15$ then go to step 2 for the next iteration.

(6) **Output:** $\bar{\gamma}_{sn}^{*}$ along with p_{sp}^{*} and p_{sn}^{*} is the obtained solution.

(2) The second step determines the approximate value for the objective function. The approximation for the SINR variable depends on the current guess starting from $\hat{\gamma}_{sn,l}$ where $l = 1$.

(3) The third step is to solve the GP approximation of (3.32) around the current guess $\hat{\gamma}_{sn,l}$ for the monomial approximation of the objective function. These monomial approximations are sufficiently accurate only in the closer neighborhood of the current guess $\hat{\gamma}_{sn,l}$. Therefore, an inequality constraint $\beta^{-1}\hat{\gamma}_{sn,l} \leq \bar{\gamma}_{sn} \leq \beta\hat{\gamma}_{sn,l}$ is added to confine the domain of variables $\bar{\gamma}_{sn}$ to a region around the current guess $\hat{\gamma}_{sn,l}$ [64]. So, the inequality constraints are sometimes called trusted region constraints [48], [64]. In most practical cases, a fixed value $\beta = 1.1$ offers a good speed/accuracy tradeoff [48].

(4) The fourth step checks whether the SINR value $\bar{\gamma}_{sn}^{*}$ that is obtained from the previous iteration has significantly been changed compared to the current guess $\hat{\gamma}_{sn,l}$. If the substantial changes satisfied the tolerance, the algorithm goes to step 6.

(5) This step took the solution as a current guess and the algorithm repeats steps $2 - 5$ until $L = 15$.

(6) The last step terminates the algorithm and took the optimal value of $\bar{\gamma}_{sn}^{*}$ with α_{sn}^{*} and p_{sn}^{*} as optimal solution. Furthermore, p_{sp}^{*} is calculated from α_{sn}^{*} using (3.29).

3.4.2 MRT: Relay to Destination

In the R-D phase, the optimization problem (3.14) can be written, after applying the lower bound of the average SINR (3.27) to replace constraint function, as

$$\min_{p_{dp},p_{dn},\bar{\gamma}_{dn}} \prod_{n=1}^{N} \lambda_{dn}^{-1} \bar{\gamma}_{dn}^{-\delta_{dn}}, \tag{3.33a}$$

$$\bar{\gamma}_{dn} \geq \frac{\frac{(M-1)\zeta_{dn}^{2}\tau_{dp}p_{dp}}{1+\zeta_{dn}\tau_{dp}p_{dp}} p_{dn}}{\frac{(M-1)\zeta_{dn}^{2}\tau_{dp}p_{dp}}{M(1+\zeta_{dn}\tau_{dp}p_{dp})} \sum\limits_{j=1,j\neq n}^{N} p_{di} + \sum\limits_{j=1}^{N} p_{dj} \frac{\zeta_{dn}}{1+\zeta_{dn}\tau_{dp}p_{dp}} + 1}, \tag{3.33b}$$

$$\tau_{dn}p_{dn} + \tau_{dp}p_{dp} \leq P_{dt}, \tag{3.33c}$$

$$0 \leq p_{dn} \leq P_{d}^{max}, \quad 0 \leq p_{dp} \leq P_{p}^{max}. \tag{3.33d}$$

Observing the optimization problem, the constraint function $(3.33b)$ is still non-convex. To make it convex, we introduce the following set of variables,

$$\alpha_{dn} = \frac{\zeta_{dn}}{1+\zeta_{dn}\tau_{dp}p_{dp}}, \quad Or, \quad \tau_{dp}p_{dp} = \frac{1}{\alpha_{dn}} - \frac{1}{\zeta_{dn}}, \tag{3.34}$$

where the range of p_{dp} is $(0, +\infty)$. So, from (3.34), we get $0 \leq \alpha_{dn} \leq \zeta_{dn}$. Substituting (3.34) into $(3.33b)$ and doing some manipulations, we get

$$\frac{M-1}{M} p_{dn}^{-1} \sum_{i=1,i\neq n}^{N} p_{di} + \frac{p_{dn}^{-1}}{\zeta_{dn}-\alpha_{dn}} \sum_{j=1}^{N} p_{dj}\alpha_{dn} + \frac{p_{dn}^{-1}}{\zeta_{dn}-\alpha_{dn}} \leq \frac{M-1}{\bar{\gamma}_{dn}}. \tag{3.35}$$

In order to further simplify (3.35), we define a new vector variable $\mathbf{b} = [b_1, b_2, \cdots b_N]$ such as

$$\frac{p_{dn}^{-1}}{\zeta_{dn}-\alpha_{dn}} \sum_{j=1}^{N} p_{dj}\alpha_{dn} + \frac{p_{dn}^{-1}}{\zeta_{dn}-\alpha_{dn}} \leq b_n, \tag{3.36}$$

$$(b_n p_{dn})^{-1} \sum_{j=1}^{N} p_{dj} \alpha_{dn} + (b_n p_{dn})^{-1} + \alpha_{dn} \leq \zeta_{dn}. \tag{3.37}$$

Substituting (3.36) into (3.35) and doing some manipulations, we have

$$\bar{\gamma}_{dn} p_{dn}^{-1} \sum_{i=1, i \neq n}^{N} p_{di} + \bar{\gamma}_{dn} \frac{M b_n}{M-1} \leq M. \tag{3.38}$$

The constraint function $(3.33c)$ can be modified, after substituting $\tau_{dn} p_{dn}$ from (3.34), as

$$\alpha_{dn}^{-1} + \tau_{dn} p_{dn} \leq P_{dt} + \zeta_{dn}^{-1}, \tag{3.39}$$

Substituting (3.37), (3.38) and (3.39) into (3.33), we can establish the final convex optimization problem for the R-D phase. Therefore, another algorithm which is similar to Algorithm 1 can be developed for the R-D phase for optimal power allocation, which is summarized as Algorithm 2.

3.5 Performance Evaluation of Proposed Algorithms

In this section, we evaluate the EE performance of the considered massive MIMO DF relay system that utilizes the proposed energy-efficient power allocation optimization strategies. We also demonstrate the accuracy of our analytical results as well as the impact of several relevant system parameters on the achievable EE via numerical simulations. The main system configurations and parameters used are summarized in Table 3.1, where we have employed typical parameter values as set in [21], [23], [43].

Assume that the relay coverage area is modeled as a disc and the relay is placed at the geometric center of the disc. Furthermore, all the source and destination UEs are assumed to be randomly and uniformly spread in the circular cell. The distance between the relay and each UE is not smaller than the minimum radius. Suppose that the orthogonal frequency-division multiplexing (OFDM) signal is transmitted. According to LTE [15], [21] we choose an OFDM symbol interval of $T_s = 71.4\mu s$ and the useful symbol duration $T_u = 66.7\mu s$. The guard interval length $T_g = 4.7\mu s$ and the total

number of symbols in each coherent time interval is given by

$$T = \frac{T_c}{T_s}\frac{T_u}{T_g} = 196. \tag{3.40}$$

Algorithm 2 Successive approximation algorithm for R-D EE maximization

(1) **Initialization:** Given tolerance $\varepsilon > 0$, parameter $\beta = 1.1$ used to control the desired approximation accuracy, and the maximum number of iterations is $L = 15$ with initial value $l = 1$. The initial value $\hat{\gamma}_{dn,l}$ for $(n = 1, 2, \cdots N)$ is obtained from the uniform power consumption in the R-D transmission link.

(2) **Computation:** Compute $\delta_{dn,l} = \hat{\gamma}_{dn,l}\left(1 + \hat{\gamma}_{dn,l}\right)^{-1}, \quad \lambda_{dn,l} = \hat{\gamma}_{dn,l}^{-\delta_{dn,l}}(1 + \hat{\gamma}_{dn,l})$.

(3) **GP Optimization:**

$$\min_{\alpha_{dn}, p_{dn}, \bar{\gamma}_{dn}} \prod_{n=1}^{N} \lambda_{dn,l}^{-1} \bar{\gamma}_{dn}^{-\delta_{dn,l}}$$

$$\bar{\gamma}_{dn} p_{dn}^{-1} \sum_{i=1, i\neq n}^{N} p_{di} + \bar{\gamma}_{dn}\frac{Mb_n}{M-1} \leq M,$$

$$\left(b_n p_{dn}\right)^{-1} \sum_{j=1}^{N} p_{dj}\alpha_{dn} + \left(b_n p_{dn}\right)^{-1} + \alpha_{dn} \leq \zeta_{dn},$$

$$\beta^{-1}\hat{\gamma}_{dn,l} \leq \bar{\gamma}_{dn} \leq \beta\hat{\gamma}_{dn,l},$$

$$\alpha_{dn}^{-1} + \tau_{dn} p_{dn} \leq P_{dt} + \zeta_{dn}^{-1},$$

$$0 \leq p_{dn} \leq P_d^{max}, \quad 0 \leq \alpha_{dn} \leq \zeta_{dn}.$$

(4) **Stopping criterion:** If $\mid \bar{\gamma}_{dn}^{*} - \hat{\gamma}_{dn,l} \mid < \varepsilon$, stop iteration, and go directly to step 6.

(5) **Setting:** Set $l = l + 1$, and update $\hat{\gamma}_{dn,l} = \bar{\gamma}_{dn}^{*}$. If $l < L$, proceed to step 2 for next iteration.

(6) **Output:** γ_{dn}^{*} together with p_{dp}^{*} and p_{dn}^{*} is the obtained solution .

To minimize the overhead of the pilot symbols, we choose the smallest quantity of training $\tau = N$. The number of symbols for S-R and R-D data transmission are assumed to be the same in one coherent time interval. In the optimization problem, the weight is assumed to be the same in both positions. In our simulation, the optimization problem in all algorithms was solved by the package CVX [49] in MATLAB.

Figure 3.1 shows the set of achievable SINR values under the initial equal power setting, i.e, $p_{sp} = p_{dp} = p_{sn} = p_{dn} = 10dB$ as compared to the optimal power scenario for four user pairs. The maximum power P_{st} and P_{dt} for S-R and R-D can be calculated from $\tau_{sp}p_{sp} + \tau_{sn}p_{sn}$ and $\tau_{dp}p_{dp} + \tau_{dn}p_{dn}$, respectively. It is obvious from Figure 3.1 that the optimal SINR is better than

Table 3.1: Simulation Parameters

Parameters	Values
Reference distance, μ_{min}	$35m$
Maximum distance, μ_{max}	$1000m$
LSF model, $\xi_n = cl_n^{\nu}$	$10^{0.53} = l_n^{3.76}$
Transmission bandwidth, B	$1.96MHz$
Coherence time, T_c	$1ms$
Coherence bandwidth, B_c	$196kHz$

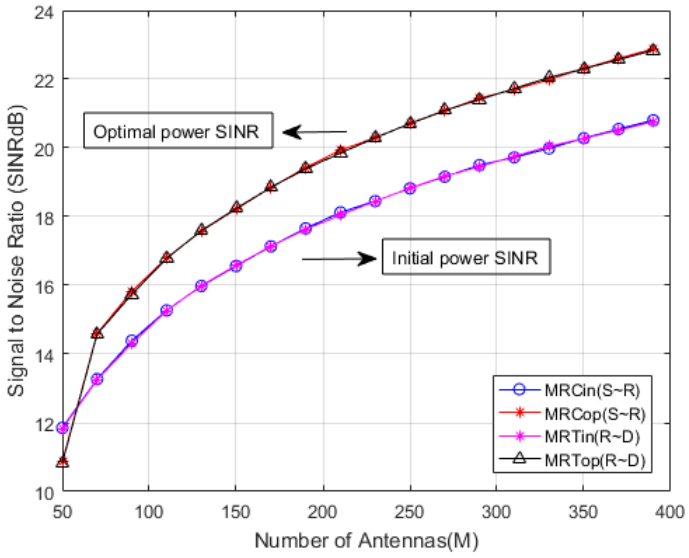

Figure 3.1: Comparison between the equal and optimal power allocations.

the initial SINR. At the beginning, the SINR of the optimal power allocation is less than the initial equal power allocation due to less number of relay antennas. This system model needs at least 50 relay antennas and the performance gets better as the number of relay antennas is increased. Hence, the analysis in section 3.4 has shown a realistic massive MIMO DF-relay systems scenario for 5G wireless communication.

In Figure 3.2, the optimal power allocation schemes are compared with the initial power allocation in terms of the EE. It is obvious that the optimal EE is better than the initial EE, especially in the case of a higher number of the relay antennas. Moreover, EE showed better performance as the number of relay antennas is increased.

Figure 3.3 showed the performance of EE versus the number of users when the number of relay

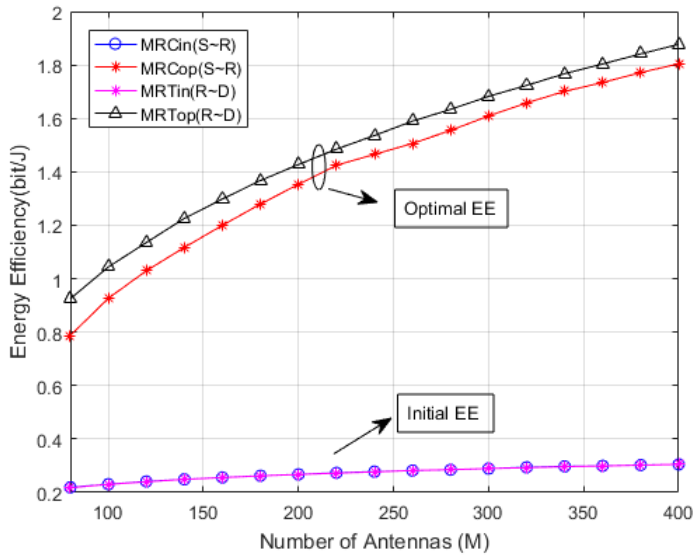

Figure 3.2: Performance of EE(bit/J) versus number of DF-relay antennas.

antennas is fixed at $M = 500$. It can be easily seen by analyzing the figure that EE is increased for a certain number of users. After that, it starts decreasing. Here the relay to destination EE outperforms the source signal to relay EE. This figure also showed the maximum number of user pairs that can be handled by this system for a certain number of relay antennas. Moreover, the performance for optimal power is still better than the initial power. This result indicates a realistic performance of this system model.

To demonstrate the advantage of our proposed algorithms as compared with an initial fixed pilot-data power allocation where the pilot and data signal have been assigned the equal power [21]. The percentage of the total power saving as for MRC/MRT schemes can be easily found from the following equations

$$\frac{N(\tau_{sp}p_{sp} + \tau_{sn}p_{sn}) - \sum_{n=1}^{N}(\tau_{sp}p^{*}_{sp} + \tau_{sn}p^{*}_{sn})}{N(\tau_{sp}p_{sp} + \tau_{sn}p_{sn})} \times 100, \tag{3.41}$$

$$\frac{N(\tau_{dp}p_{dp} + \tau_{dn}p_{dn}) - \sum_{n=1}^{N}(\tau_{dp}p^{*}_{dp} + \tau_{dn}p^{*}_{dn})}{N(\tau_{dp}p_{dp} + \tau_{dn}p_{dn})} \times 100. \tag{3.42}$$

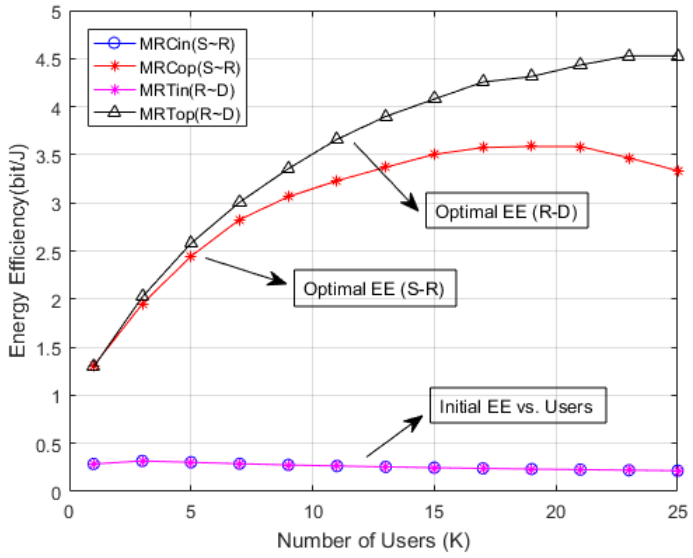

Figure 3.3: Comparison of EE(bit/J) versus number of user-pairs.

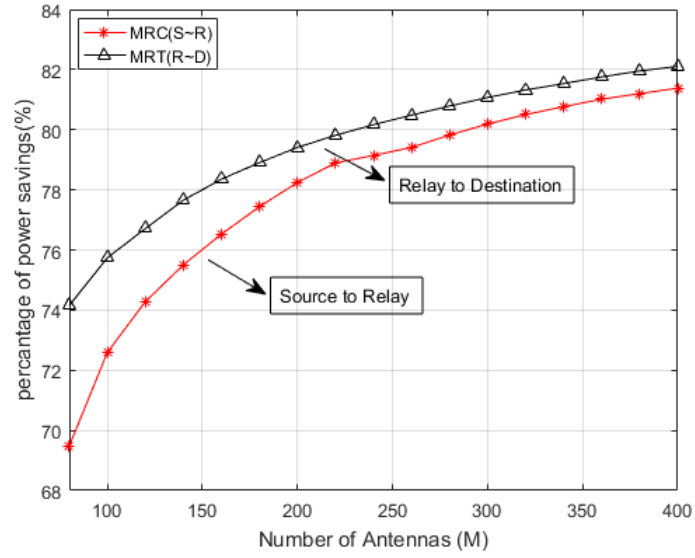

Figure 3.4: Percentages of power savings versus number of DF-relay antennas.

It can be observed from Figure 3.4 that about 69% to 81% of the total power is saved in the MRC based S-R transmission depending on the number of relay antennas used and the number of total users in the system. In the case of R-D transmission based on the MRT schemes, the system saves 74% to 82%, of the total power. The proposed power allocation schemes have a better power saving performance for a larger number of users, particularly in the high target SINR region. It should be mentioned that the benefit of deploying a large number of relay antennas tends to become marginal since the ultimate SINR performance is limited by the interference and channel estimation error.

It is to be noted that, the accuracy of the energy efficient power allocation optimization strategies for DF-relay systems is evaluated from a trusted region of SINR. This trusted region is established for the significant transmission phase for this system model. Most of the existing methods defined a fixed SINR parameter to establish the trusted region. However, they did not provide any convincing explanation about the accuracy of the SINR parameter. This thesis established the trusted region from the statistical SINR which is defined from MMSE channel estimation and uniform power allocation. Therefore, compared with existing methods, the accuracy of the simulation results in this thesis is reasonable for optimal power allocation.

3.6 Summary

This chapter has addressed the main target of this thesis where we successfully investigated the power allocation optimization problem for EE maximization. A non-convex optimization problem with the objective of EE maximization is formulated under specific QoS and transmit power constraints. To solve this challenging problem, the theory of GP is invoked to transform the original optimization problem into a convex one. In addition, a lower bound of the average SINR is introduced and utilized in the power allocation algorithms in order to simplify the proposed SINR constraints. Finally, the optimization algorithms are established using homotopy or continuation method. The obtained solution is globally optimal and all the simulation results demonstrate the effectiveness of the proposed algorithms.

Chapter 4

Global Energy Efficiency Maximization and Comparison

This chapter studies the global energy efficiency (GEE) of the desired massive MIMO DF relay system with different channel estimation schemes. In this system model, we estimate the channel using both MMSE and maximum likelihood (ML) estimation methods. We also process the signal and establish the SINR expression in equal power at S-R and R-D transmission phases. We then investigate a GEE metric defined as total sum-rate of both phases divided by the total power under different channel conditions. Two join optimization problems for power allocation are formulated under ML and MMSE channel estimation. The main objective of those optimization problems is to maximize GEE subject to the specific QoS and the transmit power constraints. A successive convex optimization technique is applied to reformulate the objective function due to non-convexity characteristics. A lower bound of the average SINR is also investigated to transform the constraint function into the standard GP format. Finally, two algorithms with different channel estimation methods are designed based on the continuation method to solve the GEE maximization problem. Simulation results are provided to demonstrate the performance evaluation of GEE of this DF relay system.

4.1 Channel Estimation and Signal Analysis

A systematic diagram as shown in Figure 2.1 of massive MIMO multi-pair one-way relay is already discussed in chapter 2. In this diagram, N pairs of users exchange their information with the help of the relay, which equipped with M antennas, and there is no direct connection between the corresponding users. Section 2.2 has discussed the antenna configuration and transmission frame structure for S-R and R-D. Channel propagation and MMSE estimation have been described in the section 2.3. In the following section, we investigate the ML channel estimation for the DF relay system.

4.1.1 Maximum Likelihood Channel Estimation

By utilizing the pilots [51], the two hop channels $\mathbf{H}_s$ and $\mathbf{H}_d$ are estimated at the relay and destination, respectively. Here, we use a part of coherence interval as a pilot symbol for the ML channel estimation. In this case, the transmitted pilot sequence of symbols for S-R and R-D phase are equal i.e, τ_{tp}, and the pilot powers for S-R and R-D phases are also equal, denoted as p_{tp}. Therefore, the received pilot signal at the relay can be written as

$$\mathbf{Y}_{rp} = \sqrt{\tau_{tp} p_{tp}} \mathbf{H}_s \mathbf{X}_p + \mathbf{W}_{rp}. \tag{4.1}$$

Here, $\mathbf{X}_p \in C^{N \times \tau_{tp}}$ is the pilot sequence transmitted from the sources, where $\mathbf{X}_p \mathbf{X}_p^H = \mathbf{I}_N$, and $\mathbf{W}_{rp}$ is AWGN matrix whose elements are i.i.d complex Gaussian $CN \sim (0, 1)$. Using the ML estimation method, the source to relay channel $\mathbf{H}_s$ is estimated as [39]-[41]

$$\hat{\mathbf{H}}_s = \frac{1}{\sqrt{\tau_{tp} p_{tp}}} \mathbf{Y}_{rp} \mathbf{X}_p^H = \mathbf{H}_s + \frac{1}{\sqrt{\tau_{tp} p_{tp}}} \mathbf{W}_{rp} \mathbf{X}_p^H \tag{4.2}$$

Let the the channel be written as $\mathbf{H}_s = \hat{\mathbf{H}}_s + \overline{\mathbf{H}}_s$. Then the estimation error can readily be written

$$\overline{\mathbf{H}}_s = \mathbf{H}_s - \hat{\mathbf{H}}_s = -\frac{1}{\sqrt{\tau_{tp} p_{tp}}} \mathbf{W}_{rp} \mathbf{X}_p^H \tag{4.3}$$

From (4.3), it can be seen that the elements of $\hat{\mathbf{H}}_s$ are independent of those of $\overline{\mathbf{H}}_s$. Both $\hat{\mathbf{H}}_s$ and

$\overline{\mathbf{H}}_s$ have i.i.d. Gaussian random elements with zero mean, and each column of matrix $\hat{\mathbf{H}}_s$ and that of $\overline{\mathbf{H}}_s$ have the same variance respectively. Let $\hat{\mathbf{h}}_{sn}$ and $\overline{\mathbf{h}}_{sn}$ denote the n-th column of the matrices $\hat{\mathbf{H}}_s$ and $\overline{\mathbf{H}}_s$ respectively, then the variance of each element in the n-th column elements of $\hat{\mathbf{H}}_s$ and $\overline{\mathbf{H}}_s$ can be expressed as

$$\sigma^2_{sn_{ML}} = \zeta_{sn} + \frac{1}{\tau_{tp} p_{tp}} \quad \text{and} \quad \xi^2_{sn_{ML}} = \frac{1}{\tau_{tp} p_{tp}}. \tag{4.4}$$

Again, the R-D channel can be estimated at the destination by using the pilots transmitted from the relay node. Using the techniques similar to those in equations (4.2) and (4.3), the ML estimation of the R-D channel can be written as $\mathbf{H}_d = \hat{\mathbf{H}}_d + \overline{\mathbf{H}}_d$, where $\hat{\mathbf{H}}_d$ and $\overline{\mathbf{H}}_d$ are statistically independent. Using (4.4), the variances of each element of n-th column elements of $\hat{\mathbf{H}}_d$ and $\overline{\mathbf{H}}_d$ can be written as

$$\sigma^2_{dn_{ML}} = \zeta_{dn} + \frac{1}{\tau_{tp} p_{tp}} \quad \text{and} \quad \xi^2_{dn_{ML}} = \frac{1}{\tau_{tp} p_{tp}}. \tag{4.5}$$

4.1.2 Sum-rates Calculation

A general signal model for multi-user massive MIMO DF relay networks operating over fading channels is presented in section 2.4, where N spatially distributed user nodes transmit their information via an intermediate relay. Recall that $\mathbf{P}_s = diag(p_{s1}, \cdots, p_{sN})$ is the power allocation matrix applied to all N source UEs and $\mathbf{P}_d = diag(p_{d1}, \cdots, p_{dN})$ is the power allocation matrix used in the relay. Let's consider both phases S-R and R-D have equal power allocation matrices such as $\mathbf{P}_s = \mathbf{P}_d = \mathbf{P}_t = diag(p_{t1}, \cdots, p_{tN})$. Therefore the SINR for S-R under MRC scheme (2.22) can be rewritten as

$$\gamma_{sn_{ML}} = \frac{p_{tn} \parallel \hat{\mathbf{h}}_{sn} \parallel^4}{\sum\limits_{i=1, i\neq n}^{N} p_{ti} \mid \hat{\mathbf{h}}^H_{sn} \hat{\mathbf{h}}_{si} \mid^2 + \sum\limits_{j=1}^{N} p_{tj} \mid \hat{\mathbf{h}}^H_{sn} \overline{\mathbf{h}}_{sj} \mid^2 + \parallel \hat{\mathbf{h}}^H_{sn} \parallel^2}. \tag{4.6}$$

where p_{tn} indicates the power of n-th user. During the R-D phase, the receive SINR is described at (2.24) for the MRT scheme. Applying the equal power similar to the S-R phase, the received SINR at the destination can be written as

$$\gamma_{dn_{ML}} = \frac{p_{tn} \| \hat{\mathbf{h}}_{dn} \|^2}{\sum\limits_{i=1, i\neq n}^{N} p_{ti} \frac{|\hat{\mathbf{h}}_{dn}^H \hat{\mathbf{h}}_{di}|^2}{\|\hat{\mathbf{h}}_{di}\|^2} + \sum\limits_{j=1}^{N} p_{tj} \frac{|\bar{\mathbf{h}}_{dn}^H \hat{\mathbf{h}}_{dj}|^2}{\|\hat{\mathbf{h}}_{dj}\|^2} + 1}. \tag{4.7}$$

Using the value of $\gamma_{sn_{ML}}$ and $\gamma_{dn_{ML}}$, we can calculate the sum-rates for S-R and R-D phase as follows

$$R_{MRC}^{ML} = \frac{1}{2} \sum_{n=1}^{N} log_2(1 + \gamma_{sn_{ML}}), \tag{4.8}$$

$$R_{MRT}^{ML} = \frac{1}{2} \sum_{n=1}^{N} log_2(1 + \gamma_{dn_{ML}}). \tag{4.9}$$

4.2 Global Energy Efficiency Maximization

The GEE measures the total performance of the DF relay system. It can be obtained from the total sum-rates for both phases divided by the total transmit power. The sum-rates for S-R and R-D transmission phase are given in (4.8) and (4.9). Therefore, we can established GEE as

$$GEE_{ML} = \frac{1}{P_{tt}} \left[R_{MRC}^{ML} + R_{MRT}^{ML} \right]$$

$$= \frac{1}{2P_{tt}} \sum_{n=1}^{N} \left[(log_2(1 + \gamma_{sn_{ML}}) + log_2(1 + \gamma_{dn_{ML}}) \right]$$

$$= \frac{1}{2P_{tt}} log_2 \left[\prod_{n=1}^{N} (1 + \gamma_{sn_{ML}})(1 + \gamma_{dn_{ML}}) \right] \tag{4.10}$$

where, (4.10) is the desired objective function for GEE maximization. The power allocation optimization problem to maximize the GEE is than formulated as

$$GEE_{ML}^{max} = \max_{p_{tp}, p_{tn}} \frac{1}{2P_{tt}} log_2 \left[\prod_{n=1}^{N} (1 + \gamma_{sn_{ML}})(1 + \gamma_{dn_{ML}}) \right] \tag{4.11a}$$

$$s.t. \quad \tau_{tp} p_{tp} + \tau_{tn} p_{tn} \leq P_{tt}, \tag{4.11b}$$

$$0 \leq p_{tn} \leq P_t^{max}, \quad 0 \leq p_{tp} \leq P_p^{max}. \tag{4.11c}$$

where P_t^{max} and P_p^{max} are the maximum power limits for each user and pilot, respectively. Since $log_2(x)$ is an increasing function of x, the objective function in (4.11) can be equivalently rewritten as

$$\min_{p_{tp},p_{tn}} \frac{1}{2P_{tt}} \left[\prod_{n=1}^{N} (1+\gamma_{sn_{ML}})^{-1} (1+\gamma_{dn_{ML}})^{-1} \right] \tag{4.12}$$

where $\frac{1}{2}$ is a multiplicative constant and P_{tt} can be measured from equal power allocation. Subtracting (4.12) into (4.11) and removing $\frac{1}{2}$, the optimization problem can be rewritten as

$$\min_{p_{tp},p_{tn}} \prod_{n=1}^{N} (1+\gamma_{sn_{ML}})^{-1} (1+\gamma_{dn_{ML}})^{-1} \tag{4.13a}$$

$$s.t. \quad \tau_{tp} p_{tp} + \tau_{tn} p_{tn} \leq P_{tt}, \tag{4.13b}$$

$$0 \leq p_{tn} \leq P_t^{max}, \quad 0 \leq p_{tp} \leq P_p^{max}. \tag{4.13c}$$

Here, (4.13) is an optimization problem subject to the inequality constraint functions. If the optimization variables p_{tp} and p_{tn} satisfy all the inequality constraints of (4.13), then they are known as feasible solution. Let, p_{tp}^* and p_{tn}^* are said to be globally optimal solutions that satisfy $p_{tp}^* \leq p_{tp}$ and $p_{tn}^* \leq p_{tn}$, respectively. Observing (4.13), the constraints are convex functions but the objective is a non-convex rational function, which is difficult to solve. Therefore, we reformulate the objective function into a convex function using CGP to facilitate its solution via simple CVX toolbox [49]. The approximation for the objective term (4.13) can be described from the lemma in chapter 3. Following by the lemma, for $\gamma_{sn_{ML}} > 0$ and $\gamma_{dn_{ML}} > 0$, the objective function $(4.13a)$ can be rewritten as

$$(1+\gamma_{sn_{ML}})^{-1} = \lambda_{sn}^{-1} {\gamma_{sn_{ML}}}^{-\delta_{sn}}, \tag{4.14}$$

$$(1+\gamma_{dn_{ML}})^{-1} = \lambda_{dn}^{-1} {\gamma_{dn_{ML}}}^{-\delta_{dn}}. \tag{4.15}$$

Here, $\gamma_{sn_{ML}}$ is approximated near an arbitrary point $\hat{\gamma}_{sn} > 0$ such as

$$\delta_{sn} = \hat{\gamma}_{sn}(1+\hat{\gamma}_{sn})^{-1}, \quad \lambda_{sn} = \hat{\gamma}_{sn}^{-\delta_{sn}}(1+\hat{\gamma}_{sn}). \tag{4.16}$$

Consequently, $\gamma_{dn_{ML}}$ is approximated near an arbitrary point $\hat{\gamma}_{dn} > 0$ such as

$$\delta_{dn} = \hat{\gamma}_{dn}(1+\hat{\gamma}_{dn})^{-1}, \quad \lambda_{dn} = \hat{\gamma}_{dn}^{-\delta_{dn}}(1+\hat{\gamma}_{dn}). \tag{4.17}$$

Substituting (4.14) and (4.15) into $(4.13a)$, the objective function can be rewritten as

$$\min_{p_{tp},p_{tn}} \prod_{n=1}^{N} \lambda_{sn}^{-1}{\gamma_{sn_{ML}}}^{-\delta_{sn}} \lambda_{dn}^{-1}{\gamma_{dn_{ML}}}^{-\delta_{dn}}. \tag{4.18}$$

Analyzing (4.18), we know that the objective function is convex. Then we can obtain optimal solution for $\gamma_{sn_{ML}}$ and $\gamma_{dn_{ML}}$. Also, p_{tp}^{*} and p_{tn}^{*} are said to be globally optimal as they are the feasible solutions of ${\gamma_{sn_{ML}}}^{*}$ and ${\gamma_{dn_{ML}}}^{*}$, respectively. Therefore, (4.6) and (4.7) can be used as a constraint function to optimize $\gamma_{sn_{ML}}$ and $\gamma_{dn_{ML}}$ variables. Including (4.6) and (4.7) as a constraint function, and substituting (4.18) into (4.13), the new optimization problem can be written as

$$\min_{p_{tp},p_{tn},\gamma_{sn_{ML}},\gamma_{dn_{ML}}} \prod_{n=1}^{N} \lambda_{sn}^{-1}{\gamma_{sn_{ML}}}^{-\delta_{sn}} \lambda_{dn}^{-1}{\gamma_{dn_{ML}}}^{-\delta_{dn}}, \tag{4.19a}$$

$$s.t. \quad \gamma_{sn_{ML}} = \frac{p_{tn} \parallel \hat{\mathbf{h}}_{sn} \parallel^4}{\sum\limits_{i=1,i\neq n}^{N} p_{ti} \mid \hat{\mathbf{h}}_{sn}^{H}\hat{\mathbf{h}}_{si} \mid^2 + \sum\limits_{j=1}^{N} p_{tj} \mid \hat{\mathbf{h}}_{sn}^{H}\overline{\mathbf{h}}_{sj} \mid^2 + \parallel \hat{\mathbf{h}}_{sn}^{H} \parallel^2}, \tag{4.19b}$$

$$\gamma_{dn_{ML}} = \frac{p_{tn} \parallel \hat{\mathbf{h}}_{dn} \parallel^2}{\sum\limits_{i=1,i\neq n}^{N} p_{ti} \frac{|\hat{\mathbf{h}}_{dn}^{H}\hat{\mathbf{h}}_{di}|^2}{\|\hat{\mathbf{h}}_{di}\|^2} + \sum\limits_{j=1}^{N} p_{tj} \frac{|\overline{\mathbf{h}}_{dn}^{H}\hat{\mathbf{h}}_{dj}|^2}{\|\hat{\mathbf{h}}_{dj}\|^2} + 1}, \tag{4.19c}$$

$$\tau_{tp}p_{tp} + \tau_{tn}p_{tn} \leq P_{tt}, \tag{4.19d}$$

$$0 \leq p_{tn} \leq P_{t}^{max}, \quad 0 \leq p_{tp} \leq P_{p}^{max}. \tag{4.19e}$$

Investigating (4.19), another new challenge appears because the right-hand sides (RHS) of the constraint functions $(4.19b)$ and $(4.19c)$ are neither monomial nor posynomial. To solve this non-convex rational functions, we introduce a lower bound of the average the SINR for our proposed

DF-relay system and, which is then used as a constraint function in (4.19) to replace the original SINR.

Here, we consider the conventional linear MRC/MRT processing for the S-R and R-D transmission for the lower bound of average SINR. In chapter three, we already introduced the lower bound of the average SINR for MMSE estimation. Similarly, we can calculate the lower bound SINR from statistical SINR (4.6) for S-R, and (4.7) for R-D under ML estimation. Therefore, following the equations (3.15)-(3.18), (4.6) can be reformulated as

$$E\left[\gamma_{sn_{ML}}\right] \geq E[\parallel \hat{\mathbf{h}}_{sn} \parallel^2] \frac{p_{tn}}{\sum\limits_{i=1,i\neq n}^{N} p_{ti}\sigma^2_{si_{ML}} + \sum\limits_{j=1}^{N} p_{tj}\xi^2_{sj_{ML}} + 1}. \tag{4.20}$$

From the ML channel estimation, we can see that $\hat{\mathbf{H}}_s$ is independent of $\overline{\mathbf{H}}_s$. The elements of the vector $\hat{\mathbf{h}}_{sn}$ are i.i.d. Gaussian random variables with zero mean and constant variance $\sigma^2_{sn_{ML}}$. Therefore, the term $\parallel \hat{\mathbf{h}}_{sn} \parallel^2$ in (4.20) can be treated as a 1×1 central complex Wishart matrix with M degrees of freedom [61] as follows

$$E[\parallel \hat{\mathbf{h}}_{sn} \parallel^2] = E[\left(\hat{\mathbf{H}}_s^H \hat{\mathbf{H}}_s\right)_{nn}] = \frac{1}{N} E[tr\left(\hat{\mathbf{H}}_s^H \hat{\mathbf{H}}_s\right)] = M\sigma^2_{sn_{ML}}. \tag{4.21}$$

Substituting (4.4) and (4.21) into (4.20), we get the final lower bound of the average SINR for S-R under the ML estimation as given by

$$E\left[\gamma_{sn_{ML}}\right] \geq \frac{M(\zeta_{sn} + \frac{1}{\tau_{tp}p_{tp}})p_{tn}}{\sum\limits_{i=1,i\neq n}^{N} p_{ti}(\zeta_{sn} + \frac{1}{\tau_{tp}p_{tp}}) + \sum\limits_{j=1}^{N} p_{tj}\frac{1}{\tau_{tp}p_{tp}} + 1}. \tag{4.22}$$

Similarly for the R-D the phase, following (3.22)-(3.26), (4.7) can be rewritten as

$$E[\gamma_{dn_{ML}}] \geq \frac{p_{tn}}{\frac{1}{M}\sum\limits_{i=1,i\neq n}^{N} p_{ti} + \frac{1}{(M-1)\sigma^2_{dn_{ML}}} \sum\limits_{j=1}^{N} p_{tj}\xi^2_{dj_{ML}} + \frac{1}{(M-1)\sigma^2_{dn_{ML}}}}. \tag{4.23}$$

Substituting (4.5) into (4.23) and performing some manipulations, the final lower bound of the average SINR for R-D under ML estimation can be written as

$$E[\gamma_{dn_{ML}}] \geq \frac{p_{tn}(M-1)(\zeta_{dn}+\frac{1}{\tau_{tp}p_{tp}})}{\frac{M-1}{M}(\zeta_{dn}+\frac{1}{\tau_{tp}p_{tp}})\sum\limits_{i=1,i\neq n}^{N} p_{ti}+\frac{1}{\tau_{tp}p_{tp}}\sum\limits_{j=1}^{N} p_{tj}+1}. \tag{4.24}$$

4.3 Proposed Algorithms for Optimal Solutions

4.3.1 GEE Algorithm with ML estimation

We first propose an algorithm for the GEE optimization problem under ML channel estimation. Investigating (4.22), we still found that the expression is non-convex. Therefore, we introduce a new set of variables

$$\alpha_{tn} = \frac{1}{\tau_{tp}p_{tp}}, \quad Or, \quad p_{tp}\tau_{tp} = \frac{1}{\alpha_{tn}}. \tag{4.25}$$

where $\alpha_{tn} \geq 0$. Substituting (4.25) into (4.22) and performing some manipulations, the S-R SINR expression can be written as

$$\bar{\gamma}_{sn_m}\sum_{i=1,i\neq n}^{N} p_{ti}p_{tn}^{-1}(\zeta_{sn}+\alpha_{tn}) + \bar{\gamma}_{sn_m}\sum_{j=1}^{N}\alpha_{tn} + \bar{\gamma}_{sn_m}p_{tn}^{-1} \leq M(\zeta_{sn}+\alpha_{tn}) \tag{4.26}$$

where $\bar{\gamma}_{sn_m} = E[\gamma_{sn_{ML}}]$ is for notational simplicity. Here, LSF cofficient changes very slowly compared with SSF and they can be reliably estimated. Assume that the LSF coefficient has a constant variance $\zeta_{sn} = 1$. Then we can get for $\alpha_{tn} \geq 0$, $1+\alpha_{tn} = \lambda_{tn}\alpha_{tn}^{\delta_{tn}}$ is approximated near an arbitrary point $\hat{\alpha}_{tn} > 0$ where $\delta_{tn} = \hat{\alpha}_{tn}(1+\hat{\alpha}_{tn})^{-1}$, and $\lambda_{tn} = \hat{\alpha}_{tn}^{\delta_{tn}}(1+\hat{\alpha}_{tn})$. Therefore, (4.26) can be reformulated as

$$\bar{\gamma}_{sn_m}\sum_{i=1,i\neq n}^{N} p_{ti}p_{tn}^{-1}\lambda_{tn} + \bar{\gamma}_{sn_m}\sum_{j=1}^{N}\alpha_{tn}^{1-\delta_{tn}} + \bar{\gamma}_{sn_m}p_{tn}^{-1}\alpha_{tn}^{-\delta_{tn}} \leq M\lambda_{tn} \tag{4.27}$$

Similar to the R-D transmission phase, (4.24) can be rewritten, after carrying out some manipulations, as

$$(M-1)M^{-1}\bar{\gamma}_{dn_m}\sum_{i=1,i\neq n}^{N} p_{ti}p_{tn}^{-1}\lambda_{tn} + \bar{\gamma}_{dn_m}\sum_{j=1}^{N}\alpha_{tn}^{1-\delta_{tn}} + \bar{\gamma}_{dn_m}p_{tn}^{-1}\alpha_{tn}^{-\delta_{tn}} \leq (M-1)\lambda_{tn} \tag{4.28}$$

where, $\bar{\gamma}_{dn_m} = E[\gamma_{dn_{ML}}]$ is applied for notational simplicity. Substituting $p_{tp}\tau_{tp}$ from (4.25) into

$(4.19d)$, we can get

$$\alpha_{tn}^{-1} + p_{tn}\tau_{tn} \leq P_{tt}. \tag{4.29}$$

Finally, substituting (4.27)-(4.29) into (4.19), the optimization problem can be rewritten as

$$\min_{\alpha_{tn}, p_{tn}, \bar{\gamma}_{sn_m}, \bar{\gamma}_{dn_m}} \prod_{n=1}^{N} \lambda_{sn}^{-1} \bar{\gamma}_{sn_m}^{-\delta_{sn}} \lambda_{dn}^{-1} \bar{\gamma}_{dn_m}^{-\delta_{dn}}, \tag{4.30a}$$

$$s.t. \quad C1 : \bar{\gamma}_{sn_m} \sum_{i=1, i\neq n}^{N} p_{ti} p_{tn}^{-1} \lambda_{tn} + \bar{\gamma}_{sn_m} \sum_{j=1}^{N} \alpha_{tn}^{1-\delta_{tn}} + \bar{\gamma}_{sn_m} p_{tn}^{-1} \alpha_{tn}^{-\delta_{tn}} \leq M \lambda_{tn}, \tag{4.30b}$$

$$C2 : (M-1) M^{-1} \bar{\gamma}_{dn_m} \sum_{i=1, i\neq n}^{N} p_{ti} p_{tn}^{-1} \lambda_{tn} + \bar{\gamma}_{dn_m} \sum_{j=1}^{N} \alpha_{tn}^{1-\delta_{tn}} + \bar{\gamma}_{dn_m} p_{tn}^{-1} \alpha_{tn}^{-\delta_{tn}} \leq (M-1) \lambda_{tn}, \tag{4.30c}$$

$$C3 : \alpha_{tn}^{-1} + p_{tn}\tau_{tn} \leq P_{tt}, \tag{4.30d}$$

$$C4 : 0 \leq p_{tn} \leq P_t^{max}, \quad 0 \leq \alpha_{tn}. \tag{4.30e}$$

Investigating (4.30), the optimization problem is now written in the standard GP format and can be solved via CVX toolbox. Further, by using (4.30), we can establish an algorithm, denoted as algorithm 3 to allocate the transmit power for both phases under ML channel estimation. This algorithm has the following steps similar to the previous algorithm in chapter 3 with a few changes:

(1) The first step initializes the algorithm, and the feasible SINR $\hat{\gamma}_{sn}$ and $\hat{\gamma}_{dn}$ are obtained from the uniform power allocation. We set a parameter $\beta > 1$ to get the desired approximation accuracy of SINR and each entry of the current SINR guess can be increased or decreased at most by a factor β. A tolerance point $\varepsilon = 0.01$ is defined here to compare between initial and optimal SINR. The algorithm starts iteration point $l = 1$ with a maximum number of iteration $L = 15$.

(2) The approximated values for the objective function λ_{sn}, δ_{sn}, λ_{dn}, δ_{dn} are determined here. The approximations for the SINR variable depend on the current guess starting from the $\hat{\gamma}_{sn,l}$ and $\hat{\gamma}_{dn,l}$, where $l = 1$.

(3) The third step is to solve the GP optimization problem (4.30) around the current guess $\hat{\gamma}_{sn,l}$

and $\hat{\gamma}_{dn,l}$ for the monomial approximation of the objective function. These monomial approximations are sufficiently accurate only in the closer neighborhood of the current guesses. Therefore, two inequality constraints $\beta^{-1}\hat{\gamma}_{sn,l} \leq \bar{\gamma}_{sn_m} \leq \beta\hat{\gamma}_{sn,l}$ and $\beta^{-1}\hat{\gamma}_{dn,l} \leq \bar{\gamma}_{dn_m} \leq \beta\hat{\gamma}_{dn,l}$ are added to confine the domain of variables $\bar{\gamma}_{sn_m}$ and $\bar{\gamma}_{dn_m}$ to a region around the current guess $\hat{\gamma}_{sn,l}$ and $\hat{\gamma}_{dn,l}$ [64], respectively. In most practical cases, a fixed value $\beta = 1.1$ offers a good speed/accuracy tradeoff [48].

(4) The fourth step checks whether the SINR value $\bar{\gamma}^*_{sn_m}$ and $\bar{\gamma}^*_{dn_m}$ that are obtained from the previous iteration has significantly been changed compared to the entries of the current guess $\hat{\gamma}_{sn,l}$ and $\hat{\gamma}_{dn,l}$. If the substantial changes satisfy the tolerance, the algorithm directly goes to step 6.

(5) This step took the solution as a current guess and the algorithm repeats steps $2-5$ until $L = 15$.

(6) The last step terminates the algorithm and output the optimal values of $\bar{\gamma}^*_{sn_m}$ and $\bar{\gamma}^*_{dn_m}$ with α^*_{tn} and p^*_{tn} as the optimal solution. Furthermore p^*_{tp} is calculated from α^*_{tn} using (4.25).

4.3.2 GEE Algorithm with MMSE estimation

The EE maximization algorithms for each transmission phase are already described in chapter 3 under MMSE channel estimation. The lower bound of the average SINR is also described for S-R and R-D transmission phase. We can use the same lower bound of the average SINR assigning $\mathbf{P}_s = \mathbf{P}_d = \mathbf{P}_t$ in both transmission phase. Therefore, the SINR expression for S-R can be defined from (3.30) such as

$$\sum_{i=1,i\neq n}^{N} \zeta_{si} p_{ti} p_{tn}^{-1} \bar{\gamma}_{sn} + p_{tn}^{-1} \bar{\gamma}_{sn} + M\alpha_{tn} + \alpha_{tn}\bar{\gamma}_{sn} \leq M\zeta_{sn}. \tag{4.31}$$

Consequently, in case of R-D transmission phase, The SINR expression can be defined from (3.37) and (3.38) for the present scenario as

Algorithm 3 Algorithm for GEE maximization under ML estimation

(1) **Initialization:** Given tolerance $\varepsilon > 0$, parameter $\beta = 1.1$ used to check the desired approximation accuracy, and the maximum number of iterations $L = 15$ with initial value $l = 1$. The initial value $\hat{\gamma}_{sn,l}$ and $\hat{\gamma}_{dn,l}$ for $(n = 1, 2, \cdots N)$ is obtained from the initial power allocation.

(2) **Computation:** Compute $\delta_{sn,l} = \hat{\gamma}_{sn,l}(1+\hat{\gamma}_{sn,l})^{-1}$, $\lambda_{sn,l} = \hat{\gamma}_{sn,l}^{-\delta_{sn,l}}(1+\hat{\gamma}_{sn,l})$ and $\delta_{dn,l} = \hat{\gamma}_{dn,l}(1+\hat{\gamma}_{dn,l})^{-1}$, $\lambda_{dn,l} = \hat{\gamma}_{dn,l}^{-\delta_{dn,l}}(1+\hat{\gamma}_{dn,l})$, respectively.

(3) **GP Optimization:**

$$\begin{aligned} \min_{\alpha_{tn}, p_{tn}, \bar{\gamma}_{sn_m}, \bar{\gamma}_{dn_m}} & \prod_{n=1}^{N} \lambda_{sn,l}^{-1} \bar{\gamma}_{sn_m}^{-\delta_{sn,l}} \lambda_{dn,l}^{-1} \bar{\gamma}_{dn_m}^{-\delta_{dn,l}}, \\ s.t. \quad & C1, C2, C3, C4, \\ & \beta^{-1}\hat{\gamma}_{sn,l} \le \bar{\gamma}_{sn_m} \le \beta\hat{\gamma}_{sn,l}, \\ & \beta^{-1}\hat{\gamma}_{dn,l} \le \bar{\gamma}_{dn_m} \le \beta\hat{\gamma}_{dn,l}. \end{aligned} \tag{4.30}$$

(4) **Stopping criterion:** If $\mid \bar{\gamma}_{sn_m}^{*} - \hat{\gamma}_{sn,l} \mid < \varepsilon$ or $\mid \bar{\gamma}_{dn_m}^{*} - \hat{\gamma}_{dn,l} \mid < \varepsilon$, stop the iteration; and directly go to step 6.

(5) **Setting:** Set $l = l + 1$, and update $\hat{\gamma}_{sn,l} = \bar{\gamma}_{sn_m}^{*}$ and $\hat{\gamma}_{dn,l} = \bar{\gamma}_{dn_m}^{*}$. If $l < L = 15$ then go to step 2 for the next iteration.

(6) **Output:** $\bar{\gamma}_{sn_m}^{*}$ and $\bar{\gamma}_{dn_m}^{*}$ along with p_{tp}^{*} and p_{tn}^{*} are the obtained solution.

$$(b_n p_{tn})^{-1} \sum_{j=1}^{N} p_{tj}\alpha_{tn} + (b_n p_{tn})^{-1} + \alpha_{tn} \le \zeta_{dn}. \tag{4.32}$$

$$\bar{\gamma}_{dn} p_{tn}^{-1} \sum_{i=1, i\neq n}^{N} p_{ti} + \bar{\gamma}_{dn} \frac{M b_n}{M-1} \le M. \tag{4.33}$$

Assuming that the LSF coefficient is also changed very slowly compared with SSF and they can be reliably estimated under MMSE estimation. For equal power allocation, (3.31) and (3.39) can be equally written as

$$\alpha_{tn}^{-1} + \tau_{tn} p_{tn} \le P_{tt} + 1, \tag{4.33).}$$

From (4.30)-(4.33), the final GEE optimization problem for MMSE channel estimation can be established as follows

$$\min_{\alpha_{tn}, p_{tn}, \bar{\gamma}_{sn}, \bar{\gamma}_{dn}} \prod_{n=1}^{N} \lambda_{sn}^{-1} \bar{\gamma}_{sn}^{-\delta_{sn}} \lambda_{dn}^{-1} \bar{\gamma}_{dn}^{-\delta_{dn}}, \tag{4.34a}$$

$$s.t. \quad D1: \sum_{i=1,i\neq n}^{N} \zeta_{si} p_{ti} p_{tn}^{-1} \bar{\gamma}_{sn} + p_{tn}^{-1} \bar{\gamma}_{sn} + M\alpha_{tn} + \alpha_{tn}\bar{\gamma}_{sn} \leq M\zeta_{sn}, \tag{4.34b}$$

$$D2: (b_n p_{tn})^{-1} \sum_{j=1}^{N} p_{tj}\alpha_{tn} + (b_n p_{tn})^{-1} + \alpha_{tn} \leq \zeta_{dn}, \tag{4.34c}$$

$$D3: \bar{\gamma}_{dn} p_{tn}^{-1} \sum_{i=1,i\neq n}^{N} p_{ti} + \bar{\gamma}_{dn} \frac{Mb_n}{M-1} \leq M, \tag{4.34d}$$

$$D4: \alpha_{tn}^{-1} + \tau_{tn} p_{tn} \leq P_{tt} + 1, \tag{4.34e}$$

$$D5: 0 \leq p_{tn} \leq P_t^{max}, \quad 0 \leq \alpha_{tn}. \tag{4.34f}$$

Based on the above optimization problem, we can further establish a GEE algorithm to obtain the optimal solution under MMSE channel estimation.

Algorithm 4 Algorithm for GEE maximization under MMSE estimation

(1) **Initialization:** Given tolerance $\varepsilon > 0$, parameter $\beta = 1.1$ used to check the desired approximation accuracy, and the maximum number of iterations $L = 15$ with initial value $l = 1$. The initial value $\hat{\gamma}_{sn,l}$ and $\hat{\gamma}_{dn,l}$ for $(n = 1, 2, \cdots N)$ is obtained from the initial power allocation.

(2) **Computation:** Compute $\delta_{sn,l} = \hat{\gamma}_{sn,l}(1+\hat{\gamma}_{sn,l})^{-1}$, $\lambda_{sn,l} = \hat{\gamma}_{sn,l}^{-\delta_{sn,l}}(1+\hat{\gamma}_{sn,l})$ and $\delta_{dn,l} = \hat{\gamma}_{dn,l}(1+\hat{\gamma}_{dn,l})^{-1}$, $\lambda_{dn,l} = \hat{\gamma}_{dn,l}^{-\delta_{dn,l}}(1+\hat{\gamma}_{dn,l})$, respectively.

(3) **GP Optimization:**

$$\begin{aligned} &\min_{\alpha_{tn}, p_{tn}, \bar{\gamma}_{sn}, \bar{\gamma}_{dn}} \prod_{n=1}^{N} \lambda_{sn,l}^{-1} \bar{\gamma}_{sn}^{-\delta_{sn,l}} \lambda_{dn,l}^{-1} \bar{\gamma}_{dn}^{-\delta_{dn,l}}, \\ &s.t. \quad D1, D2, D3, D4, D5 \\ &\beta^{-1}\hat{\gamma}_{sn,l} \leq \bar{\gamma}_{sn} \leq \beta\hat{\gamma}_{sn,l}, \\ &\beta^{-1}\hat{\gamma}_{dn,l} \leq \bar{\gamma}_{dn} \leq \beta\hat{\gamma}_{dn,l}. \end{aligned} \tag{4.34}$$

(4) **Stopping criterion:** If $\mid \bar{\gamma}_{sn}^{*} - \hat{\gamma}_{sn,l} \mid < \varepsilon$ or $\mid \bar{\gamma}_{dn}^{*} - \hat{\gamma}_{dn,l} \mid < \varepsilon$, stop the iteration; and directly go to step 6.

(5) **Setting:** Set $l = l + 1$, and update $\hat{\gamma}_{sn,l} = \bar{\gamma}_{sn}^{*}$ and $\hat{\gamma}_{dn,l} = \bar{\gamma}_{dn}^{*}$. If $l < L = 15$ then go to step 2 for the next iteration.

(6) **Output:** $\bar{\gamma}_{sn}^{*}$ and $\bar{\gamma}_{dn}^{*}$ along with p_{tp}^{*} and p_{tn}^{*} is the obtained solution.

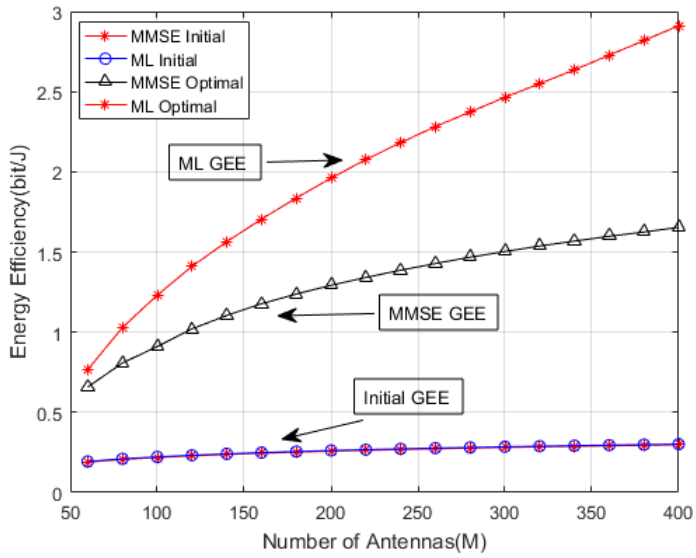

Figure 4.1: Comparison of GEE under different channel estimation schemes.

4.4 Performance Analysis of Optimal Solutions

We evaluated the GEE performance in this section for the considered massive MIMO DF relay system. The system performance under different channel estimation schemes and a detailed comparison will be shown. We use the similar parameter setting as in the previous chapter for the simulation.

In Figure 4.1, the optimal power allocation schemes are compared with the initial power allocation schemes in terms of the GEE. It is obvious that the optimal GEE is better than the initial GEE, especially in the case of a higher number of the relay antennas. Moreover, GEE showed better performance as the number of relay antennas increased. In this MIMO DF relay system, GEE under ML shows the better performance than the system under the MMSE channel condition. It can also be observed that the GEE performances of both ML and MMSE approaches are getting large as the relay antenna gets very large. Both optimal GEE outperform the initial GEE.

The advantages of our proposed algorithms as compared with an initial pilot-data power allocation are described in Figure 4.2. The percentage of the total power saving for MRC/MRT schemes under different channel conditions can be found from the figure. It can be observed that about 68%

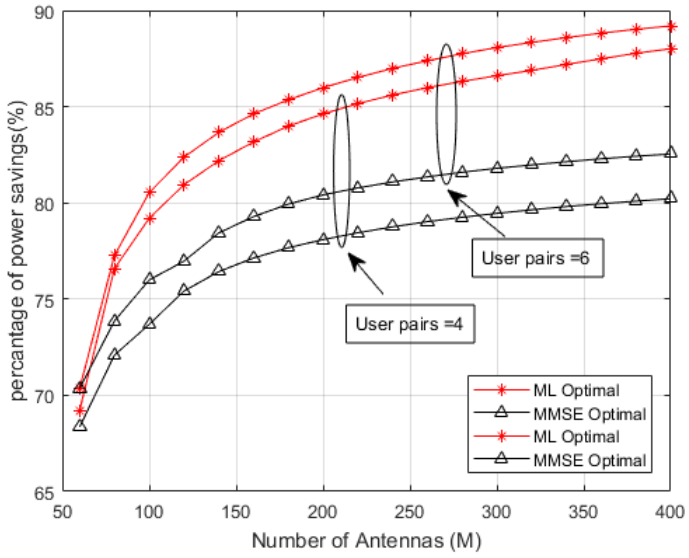

Figure 4.2: Power savings under different number of user pairs.

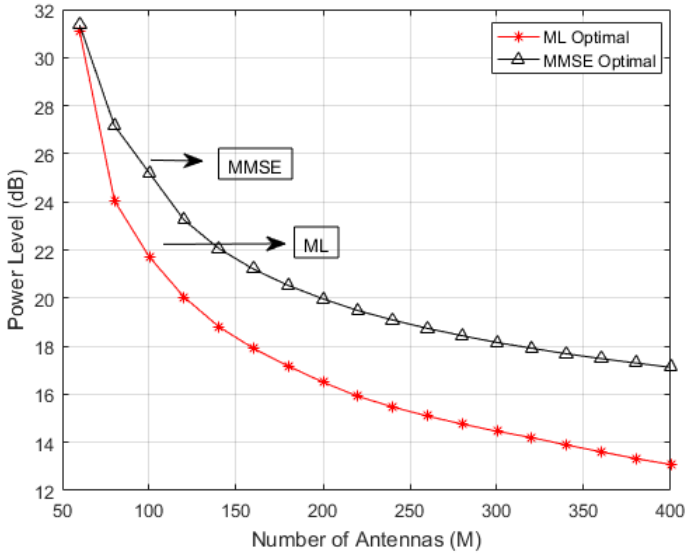

Figure 4.3: Optimal power allocation vs. number of relay antennas.

to 81% of the total power is saved under MMSE estimation depending on the number of relay antennas used in the case of four user pairs. In the case of ML estimation, the system saves 69% to 87%, of the total power. The proposed power allocation schemes have a better power saving performance for a larger number of users. It should be mentioned that the benefit of deploying a large number of relay antennas tends to become marginal since the ultimate SINR performance is limited by the interference and channel estimation error. Figure 4.3 showed the total power for all users versus the number of relay antennas. It is obvious that as M grows, the power decreases for both channel estimation schemes which indicates that the use of massive MIMO can save a great deal of transmit power.

In this thesis, the GEE indicates an end-to-end effect which was achieved from the total sum-rate divided by the total power. This system formulation has less complexity than that using the GEE based on $min(.)$ function which returns the smaller rate of the two transmission phases. It also provides better accuracy due to the predefined trusted region of SINR for each transmission phase for optimal power allocation. This GEE system model can investigate the optimal power for each transmission phase. Moreover, we can easily extend this system model into more transmission phases for multi-hop relay transmissions.

4.5 Summary

This chapter has delt with the GEE maximization of DF relay systems where GEE is defined as the total sum-rates divided by the total transmit power. First, we have investigated the channel estimation using the principle of ML. The accurate closed-form expression for GEE is derived and an optimization problem is established to maximize GEE for the overall system. The objective function of the optimization problem is the expression of GEE which is non-convex. Therefore, an approximate convex problem is formulated and the SINR constraint functions are transformed to a standard GP format by using a lower bound of the SINR. Finally, two algorithms are designed under different channel estimation schemes based on homotopy method. Matlab simulations are carried out to evaluate the performance comparison of GEE.

Chapter 5

Conclusion

5.1 Thesis Summary

In this thesis, a massive MIMO aided cooperative DF-relay system has been considered as a small-cell sub-system of a macro cellular system. These small cells can be deployed in the border or the edge of a macro cell where there are few and infrequent users. A multi-pair one-way communication system is described where a pair of user's can communicate with each other via DF-relay. Due to the popularity of AF-relay system, most of the existing works have considered AF-relay for signal transmission. However, AF relay system accumulated the transmit signal blindly with noise and fading along the transmission path. For this reason, the system performance is degraded by error at the relay which is propagated to the destination. There has been a significant interest in investigating energy efficiency (EE) of AF relay because the EE can not be investigated in particular phase for AF relay. Moreover, the CSI is imperfect and even unavailable in case of AF-relay systems. In addition, EE and global energy efficiency (GEE) investigation is often treated as the power allocation optimization problem. Most of the time, the optimization problem is difficult to solve due to the non-convexity characteristics. Therefore, DF-relay is introduced to overcome the above discussed problem at AF-relay. An MMSE and ML criterion can easily be applied at DF-relay for channel estimation and some numerical optimization methods are applied to solve the non-convexity. Compared to AF-relay, EE and GEE investigation is much easier due to dividing the transmission phase and applied CSI in this thesis system model.

The main achievement of this thesis is to establish a novel algorithm for the transmission phase to improve the EE by allocating the optimal power. A linear combining method MRC is applied at the relay and MRT is used to forward the signals from relay to destinations. Then SINR is calculated for MRC/MRT based on initial power allocation and the EE metrics for both transmission phases are investigated which are the main objective functions for the EE maximizing optimization problem. A non-convex power allocation optimization problem is formulated based on the QoS and transmit power constraints. To make it convex function, a few numerical optimization techniques such as GP, CGP are applied to convert the objective function to an equivalent to the sequence of GP which can be easily solved by CVX tools. A lower bound of the average SINR is also discussed to reformulate the subjective function in standard GP format. Finally, an algorithm is designed for each transmission phase based on homotopy or continuation method. This algorithm has significantly reduced the transmit power and increased the system performance by improving EE. Different criteria including the percentage of power increment, and increasing number of users have been used to evaluate the performance of the new method. These new method has also reduced the computational complexity by investigating EE maximization in each transmission phase.

Another algorithm is proposed to show the join transmission for both phases to investigate GEE. This investigation is done under different channel estimation schemes. For this, we have investigated the ML channel estimation. A closed-form expression for GEE is also derived and applied as an objective function in GEE maximization problem. CGP are used to reformulate the objective function as a sequence of GP and a lower bound of the average SINR is also derived to convert the subjective function into the standard GP format. The performance of GEE is showed in both channel conditions and a detailed comparison indicates that the GEE under ML outperform the GEE under MMSE channel estimation. The optimal GEE under both channel estimation conditions is better than that of the initial GEE calculated from fixed pilot-data power allocation. The performance of the proposed method is also evaluated for the different numbers of user criteria where the greater number of users outperforms the case of less number of users. Moreover, the performance is better for more relay antennas which validates the framework of merging massive MIMO with cooperative relay systems in this paper.

5.2 Future Works

The contributions presented in this thesis for relay communication system can be extended or used to explore some new research topics. In particular, some of the recommendations for future work are as follows

- *New approaches of relaying*

  AF and DF-relay performance analysis is the main topic of this thesis. Despite that, there are some new emerging proposals for the further improvements of relaying such as selective, hybrid, incremental relaying etc. Selective relaying can adapt the current conditions of the communication channels and apply a certain predetermined threshold to measure the signal for forwarding [65]. Hybrid relay communication system is specially designed for joint AF and DF relay [66]. The incremental relay technique is evaluated to increase SE using a feedback from the destination to indicate the relay to send the signal only when it is necessary [67]. Merging massive MIMO with this new relaying approaches including multi-hop relaying might be the future development of research.

- *Other linear processing techniques*

  Linear processings techniques have received a wide attention due to spectrum scarcity, low implementation complexity, and satisfactory performance. In this thesis, we have only applied MRC/MRT; there are few other linear techniques such as ZF, MMSE which are worth further study. It might significantly improve the performance of MRC/MRT and open a new door of research for this system model.

- *Circuit power consideration*

  In this thesis, we investigated the transmit power consumption with specific QoS, whereas the circuit power consumption is fixed. The circuit power is one of the most important factors for power allocation optimization problem for maximizing EE [23]. We cannot evaluate the perfect EE without considering circuit power. Nowadays, a lot of research activities focused on circuit power and design many system power consumption model. Therefore, future research trend for EE improvement depends on total power consumption model including transmit and

circuit power for accurate performance.

- *Relay for secure communication*

  This thesis considered the relays are build in fixed infrastructure. In a practical scenario, a fixed relay is expected not to work well in providing secure communications because both legitimate users and eavesdroppers are not static. One possible solution to this problem is to deploy vehicular relays [68], [69]. In particular, the mobile relays can flexibly move their positions and select different secrecy schemes. However, it is still an open issue to design mobile relays to facilitate secure communications. The research challenges are two-fold, namely, the mobile relays require the knowledge of the eavesdroppers to adjust their positions and more signaling overhead is required for multiple relay cooperation.

Appendix A

Convex Sets and Convex Functions

A.1 Convex Sets

A set $C \subseteq \mathbf{R}^n$ is affine if the line through any two distinct points in C lies in C, i.e.,$\forall x_1, x_2 \in C$ and $\theta \in \mathbf{R}$, we have $\theta x_1 + (1-\theta)x_2 \in C$. Figure A.1 gives an example of an affine set. The line segment between x_1 and x_2 corresponds to θ between 0 and 1. Affine set contains the linear combination of any two points in C provided the cofficients in the linear sum to one.

A set C is convex if the line segment between any two points in C lies entirely in C, i.e., $\forall x_1, x_2 \in C$ and any $0 \leq \theta \leq 1$, we have $\theta x_1 + (1-\theta)x_2 \in C$. Figure A.2 illustrates examples of convex and non-convex sets. The hexagon and the circle are convex, whereas the boomerang is not. The line segment between the two points in the "boomerang" set (shown as dots) is not contained in the set. Roughly speaking, a set is convex if every point in the set can be seen by every other point along a straight path between them lying in the set. Every affine set also convex, since

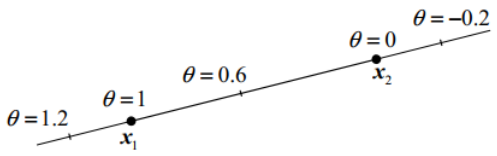

Figure A.1: Example of an affine set: a line passing through x_1 and x_2. Any point is described by $\theta x_1 + (1-\theta)x_2$, where θ varies over $\mathbf{R}$ on the line.

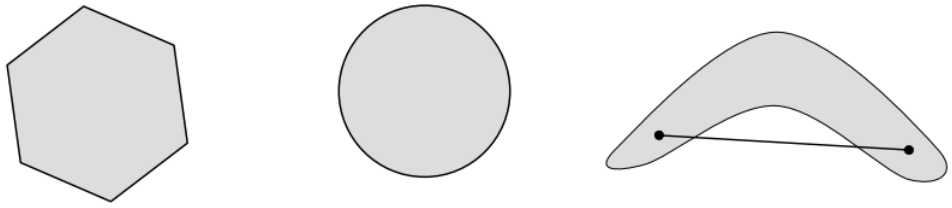

Figure A.2: Examples of convex and non-convex sets.

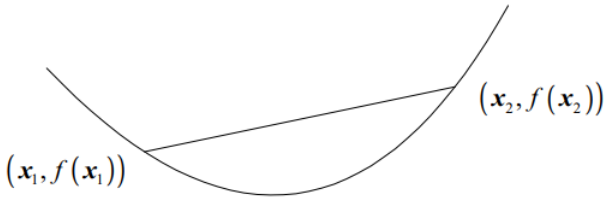

Figure A.3: Graph of a convex function. The line segment between any two points on the graph lies above the graph.

it contains the entire line between any two distinct points in it. Therefore, the line segment is also between the points.

A.2 Convex Functions

A function $f : \mathbf{R}^n \in \mathbf{R}$ is convex if the domain where f is defined, denoted as **dom** f is a convex set for all $x_1, x_2 \in$ **dom** f, and θ with $0 \leq \theta \leq 1$, we have

$$f(\theta x_1 + (1-\theta)x_2) \leq \theta f(x_1) + (1-\theta)f(x_2). \tag{A.1}$$

In geometric visualization, the inequality means that the graph segment of the function f between $(x_1, f(x_1))$ and $(x_2, f(x_2))$ is strictly below the line segment connecting the two points. Figure A.3 is showed for an illustration. A function f is said to be concave if $-f$ is a convex function. Therefore, a function is convex if and only if it is convex when restricted to any line that interests its domain. Besides the definition of a convex function, there are several ways to verify the convexity of a function f:

- *First order condition*: if f is differentiable, i.e., the gradient of f:

$$\bigtriangledown f(x) = \left(\frac{\partial f}{\partial x_1}, \frac{\partial f}{\partial x_2}, \cdots, \frac{\partial f}{\partial x_n} \right)$$

exists at each $x \in \textbf{dom} \quad f$, the first order condition states that f is convex if and only if

$$f(y) \geq f(x) + \bigtriangledown f(x)^T (y - x), \quad for \quad all \quad y \in \textbf{dom} \quad f. \tag{A.2}$$

- *Second order condition*: if f is twice-differentiable, i.e., the Hessian $\bigtriangledown^2 f(x)$:

$$\bigtriangledown^2 f(x)_{ij} = \frac{\partial^2 f(x)}{\partial x_i \partial x_j}$$

exists at each $x \in \textbf{dom} \quad f$, the second order condition states that f is convex if and only if

$$\bigtriangledown^2 f(x) \geq 0, \quad for \quad all \quad x \in \textbf{dom} \quad f. \tag{A.3}$$

Therefore, f is obtained from simpler convex functions by operations that preserves convexity, such as: non-negative weighted sum, composition of affine function, pointwise maximum and supremum, minimization, and perspective.

Appendix B

Other Mathematical Methods

B.1 Homotopy or Continuation Method

Homotopy method belongs to the family of continuation methods called homotopy continuation methods. The concept of homotopy is a mathematical formulation of the intuitive idea of a continuous deformation from one geometrical configuration to other in the sense that this concept formalizes the naive idea of continuous deformation of a continuous map [50]. All the continuation methods represent a way to find a solution to a problem by constructing a new problem, which is simpler than the original one. Afterwards, it gradually deforms this simpler problem into the original one keeping track of the series of zeros that connect the solution of the simpler problem to that of the original harder one. The greatest advantage of the homotopy methods is that they offer a way to have a globally convergent method to find the zeros of any function $f : \mathbf{R}^k \rightarrow \mathbf{R}^k$ [59].

Let X and Y be the topological spaces and $I = [0, 1]$ be the closed unit interval with topology induced by the natural topology on the real line $\mathbf{R}$. The function $F : \mathbf{R}^{n+1} \rightarrow \mathbf{R}^n$ is called the homotopy function. The two continuous maps g, $f : X \rightarrow Y$ (or g is said to be homotopic f) are said to be homotopic if there exists a continuous map $F : X \times I \rightarrow Y$. In other words, the objective of continuously deforming a function g into f can be any continuous function such that: $F(x, 0) = g(x)$ and $F(x, 1) = f(x)$. Hence we construct $F(x, 0)$ in such a way that its zeros are easily found while we also require that, F coincides with the original function f once the parameter is equal to 1.

B.2 Jensen's Inequality

Consider a function $f : I \to \mathbf{R}$, where *I* is an interval in **R**. We say that f is a convex function if, for any two points x and y in *I* and any $\theta \in [0, 1]$, we have

$$f(\theta x + (1 - \theta)y) \leq \theta f(x) + (1 - \theta)f(y). \tag{B.1}$$

We say that f is concave if

$$f(\theta x + (1 - \theta)y) \geq \theta f(x) + (1 - \theta)f(y). \tag{B.2}$$

Note that in the above definition, the term $\theta x + (1 - \theta)y$ is the weighted average of x and y. Also, $\theta f(x) + (1 - \theta)f(y)$ is the weighted average of $f(x)$ and $f(y)$. More generally, for a convex function $f : I \to \mathbf{R}$, and $x_1, x_2, \cdots, x_n$ in *I* and non-negative real numbers θ_i such that $\theta_1 + \theta_2 + ... + \theta_n = 1$, we have

$$f(\theta_1 x_1 + \theta_2 x_2 + \cdots + \theta_n x_n) \leq \theta_1 f(x_1) + \theta_2 f(x_2) + \cdots + \theta_n f(x_n). \tag{B.3}$$

If $n = 2$, the statement $(B.3)$ is the definition of convex functions. You can extend it to higher values of n by induction. Now, consider a discrete random variable X with n possible values $x_1, x_2, \cdots, x_n$. In Equation $(B.3)$, we can choose $\theta_i = P(X = x_i) = P_X(x_i)$. Then, the left-hand side of $(B.3)$ becomes $f(E[X])$ and the right-hand side becomes $E[f(X)]$. So we can prove the Jensen's inequality in this case. Using limiting arguments, this result can be extended to other types of random variables.

If $f(x)$ is a convex function on R_X, and $E[f(X)]$ and $f(E[X])$ are finite, then we can write the above inequality as $E[f(X)] \geq f(E[X])$.

To use Jensen's inequality, we need to determine if a function f is convex. A useful method is the second derivative. A twice-differentiable function $f : I \to \mathbf{R}$ is convex if and only if $f"(x) \geq 0$ for all $x \in I$. For example, if $g(x) = x^2$, then $g"(x) = 2 \geq 0$, thus $g(x) = x^2$ is convex over **R**.

B.3 Wishart Matrices

The $m \times m$ random matrix $\mathbf{A} = \mathbf{H}\mathbf{H}^H$ is a (central) real/complex Wishart matrix with n degrees of freedom and covariance matrix $\mathbf{a}$, such as $(\mathbf{A} \sim W_m(n, \mathbf{a}))$. If the columns of the $m \times n$ matrix $\mathbf{H}$ are zero-mean independent real/complex Gaussian vectors with covariance matrix $\mathbf{a}$ then the p.d.f. of a complex Wishart matrix $(\mathbf{A} \sim W_m(n, \mathbf{a}))$ for $n \geq m$ is

$$f_{\mathbf{A}}(\mathbf{B}) = \frac{\pi^{-m(m-1/2)}}{det\mathbf{a}^n \prod_{i=1}^{m}(n-i)!} exp[-tr(\mathbf{a}^{-1}\mathbf{B})] det\mathbf{B}^{n-m}. \tag{B.4}$$

The properties of the first and second order moments of a central Wishart matrix and its inverse as following

For a central Wishart matrix $(\mathbf{W} \sim W_m(n, \mathbf{I}))$

$$E[tr(\mathbf{W})] = mn, \tag{B.5}$$

$$E[tr(\mathbf{W}^2)] = mn(m+n), \tag{B.6}$$

$$E[tr^2(\mathbf{W})] = mn(mn+1). \tag{B.7}$$

For a central Wishart matrix $(\mathbf{W} \sim W_m(n, \mathbf{I}))$ with $n > m$

$$E[tr(\mathbf{W}^{-1})] = \frac{m}{(n-m)} \tag{B.8}$$

References

[1] C.-L. I, C. Rowell, S. Han, Z. Xu, G. Li, and Z. Pan, "Toward green and soft: A 5G perspective," *IEEE Communication Magazine*, volume 52, pages 66-73, Feb 2014.

[2] "Global Mobile Data Traffic Forecast Update 2012-2017," *Cisco Visual Networking Index*, Feb 2013.

[3] M. Ismail, and W. Zhuang, "Network cooperation for energy saving in green radio communications," *IEEE Wireless Commununication Magazine*, volume 18, pages 76-81, Oct 2011.

[4] Z. Hasan, H. Boostanimehr, and V. Bhargava, "Green cellular networks: A survey, some research issues and challenges," *IEEE Communication Surveys and Tutorials*, volume 13, pages 524-540, Apr 2011.

[5] X. Cao, L. Liu, Y. Cheng, and X. S. Shen, "Towards Energy-Efficient Wireless Networking in the Big Data Era: A Survey," *IEEE Communications Surveys and Tutorials*, volume 20, pages 303-332, year 2018.

[6] J. G. Proakis, "Digital Communication," 5th edition, *McGraw-Hill, New york*, year 2008.

[7] I. Krikidis, and G. Zheng, "Advance relay technologies in next generation wireless communications," *IET publishers*, year 2015.

[8] A. Nosratinia, T. E. Hunter, and A. Hedayat, "Cooperative communication in wireless networks," *IEEE Communication Magazine*, volume 42, pages 74-80, Oct 2004.

[9] "Air Interface for Broadband Wireless Access Systems - Amendment 1: Multihop Relay Specification," *IEEE Standard 802.16j*, Jun 2009.

[10] F. Boccardi, R. Heath, A. Lozano, T. Marzetta, and P. Popovski, "Five disruptive technology directions for 5G," *IEEE Communication Magazine*, volume 52, pages 74-80, Feb 2014.

[11] T. Cover, and A. E. Gamal, "Capacity theorems for the relay channel," *IEEE Transactions on Information Theory*, volume 25, pages 572-584, year 1979.

[12] Y. Fan, and J. Thompson, "MIMO configurations for relay channels: Theory and practice," *IEEE Transactions on Wireless Communications*, volume 6, pages 1774-1786, May 2007.

[13] M. Yuksel, and E. Erkip, "Multiple-antenna cooperative wireless systems: A diversity-multiplexing tradeoff perspective," *IEEE Transactions on Information Theory*, volume 53, pages 3371-3393, Oct 2007.

[14] Y.Yang, H. Hu, J. Xu, and G. Mao, "Relay technologies for WiMAX and LTE advanced mobile systems," *IEEE Communication Magazine*, volume 47, pages 100-105, Oct 2009.

[15] K. Loa, C. -C. Wu, S. -T. Sheu, Y. Yuan, M. Chion, D. Huo, and L. Xu "IMT-advanced relay standards [WiMAX/LTE Update]" *IEEE Communication Magazine*, volume 48, pages 40-48, Aug 2010.

[16] G. Kramer, I. Maric, and R. D. Yates, "Cooperative communications," *Foundations and Trends in Networking*, volume 1, year 2006.

[17] C. S. Patel, and G. L. Stuber, "Channel estimation for amplify and forward relay based cooperation diversity systems," *IEEE Transactions on Wireless Communications*, volume 6, pages 2348-2356, year 2007.

[18] T. Himsoon, W. P. Siriwongpairat, W. Su, and K. J. R. Liu, "Differential modulation with threshold based decision combining for cooperative communications," *IEEE Transactions on Signal Processing*, volume 55, pages 3905-3923, year 2007.

[19] E. C. van der Meulen, "Three terminal communication channels," *Advances in Applied Probability*, volume 3, pages 120-154, year 1971.

[20] E. Dahlman, S. Parkvall, J. Skld, and P. Beming, "3G Evolution HSPA and LTE for Mobile Broadband," *New York: Academic*, year 2008.

[21] H. Q. Ngo, E. Larsson, and T. Marzetta, "Energy and spectral efficiency of very large multiuser MIMO systems," *IEEE Transactions on Communications*, volume 61, pages 1436-1449, Apr 2013.

[22] L. Lu, G. Y. Li, A. L. Swindlehurst, A. Ashikhmin, and R. Zhang, "An overview of massive MIMO: Benefits and challenges," *IEEE Journal of Selected Topics in Signal Processing*, volume 8,

pages 742-758, May 2014.

[23] E. Bjrnson, L. Sanguinetti, J. Hoydis, and M. Debbah, ”Optimal design of energy-efficient multi-user MIMO systems: Is massive MIMO the answer?,” *IEEE Transactions on Wireless Communications*, volume 14, pages 3059-3075, Jun 2015.

[24] J. Joung, and A. Sayed, ”Multiuser two-way amplify-and-forward relay processing and power control methods for beamforming systems,” *IEEE Transactions on Signal Processing*, volume 58, pages 1833-1846, Mar 2010.

[25] M. Tao, and R. Wang, ”Linear precoding for multi-pair two-way MIMO relay systems with max-min fairness,” *IEEE Transactions on Signal Processing*, volume 60, pages 5361-5370, Oct 2012.

[26] D. Gund uz, and E. Erkip, ”Opportunistic cooperation by dynamic resource allocation,” *IEEE Transactions on Wireless Communications*, volume 6, pages 1446-1454, Apr 2007.

[27] Y. Liang, V. V. Veeravalliand, and H. V. Poor, ”Resource allocation for wireless fading relay channels: Max-min solution,” *IEEE Transactions on Information Theory*, volume 53, pages 3432-3453, Oct 2007.

[28] H. A. Suraweera, H. Q. Ngo, T. Q. Duong, C. Yuen, and E. G. Larsson, ”Multi-pair amplify-and-forward relaying with very large antenna arrays,” *IEEE International Conference on Communications (ICC)*, Budapest, Hungary, pages 1-6, Jun 2013,

[29] H. Cui, L. Song, and B. Jiao, ”Multi-pair two-way amplify-and-forward relaying with very large number of relay antennas,” *IEEE Transactions on Wireless Communications*, volume 13, pages 2636-2645, May 2014.

[30] S. Jin, X. Liang, K.-K. Wong, X. Gao, and Q. Zhu, ”Ergodic rate analysis for multipair massive MIMO two-way relay networks,” *IEEE Transactions on Wireless Communications*, volume 14, pages 1480-1491, Mar 2015.

[31] Z. Zhang, Z. Chen, M. Shen, and B. Xia, ”Spectral and energy efficiency of multipair two-way full-duplex relay systems with massive MIMO,” *IEEE Journal on Selected Areas in Communications*, volume 34, pages 848-863, Apr 2016.

[32] J. S. Lemos, F. Rosrio, F. A. Monteiro, J. Xavier, and A. Rodrigues, ”Massive MIMO full-duplex relaying with optimal power allocation for independent multipairs,” *IEEE 16th International*

Workshop on Signal Processing Advances in Wireless Communications (SPAWC), Stockholm, Sweden, pages 306-310, Jun 2015.

[33] E. Sharma, R. Budhiraja, K. Vasudevan, and L. Hanzo, "Full-Duplex Massive MIMO Multi-Pair Two-Way AF Relaying: Energy Efficiency Optimization," *IEEE Transactions on Communications*, pages 1 - 1, Year 2018.

[34] X. Xia, Y. Xu, K. Xu, D. Zhang, and W. Ma, "Full-duplex massive MIMO AF relaying with semi-blind gain control, *IEEE Transactions on Vehicular Technology*, volume 65, pages 5797-5804, year 2015.

[35] Y. Dai, and X. Dong, "Power allocation for multi-pair massive MIMO two-way AF relaying with linear processing," *IEEE Transactions on Wireless Communications*, volume 15, pages 5797 - 5804, year 2016.

[36] K. Lee, H. M. Kwon, J. Yang, E. M. Sawan, and H. Park, "Two-Way AF MIMO Beamforming Relay Strategies under Transmit Power Constraint," *IEEE Military Communications Conference (MILCOM)*, San Diego, CA, pages 533-537, year 2013.

[37] Y. Dai, and X. Dong, "Power Allocation for Multi-Pair Massive MIMO Two-Way AF Relaying With Linear Processing," *IEEE Transactions on Wireless Communications*, volume 15, pages 5932 - 5946, Year 2016.

[38] S. Gong, C. Xing, N. Yang, Y. -C. Wu, and Z. Fei, "Energy Efficient Transmission in Multi-User MIMO Relay Channels With Perfect and Imperfect Channel State Information," *IEEE Transactions on Wireless Communications*, volume 16, pages 3885 - 3898, Year 2017.

[39] J. Wang, O. Wen, and S. Li, "Soft-output MMSE V-BLAST detector under ML channel estimation and channel correlation," *IEEE Communication Letter*, volume 13, pages 211-214, year 2009.

[40] B. Zarikoff, and J. Cavers, "Coordinated multi-cell systems: carrier frequency offset estimation and correction," *IEEE Journal for Setect Areas communication*, volume 13, pages 1490-1501, year 2009.

[41] P. Li, D. Paul, R. Narasimhan, and J. Cioffi, "On the distribution of SINR for the MMSE MIMO receiver and performance analysis," *IEEE Transactions on Information Theory*, volume 52, pages 271-286, year 2006.

[42] J. N. Laneman, D. Tse, and G. Wornell, ”Cooperative diversity in wireless networks: Efficient protocols and outage behavior,” *IEEE Transactions on Information Theory*, volume 50, pages 3062-3080, Dec 2004.

[43] F. Tan, T. Lv, and S. Yang, ”Power Allocation Optimization for Energy-Efficient Massive MIMO Aided Multi-Pair Decode-and-Forward Relay Systems,” *IEEE Transactions on Communicatons*, Volume 65, pages 2368-2381, Year 2017.

[44] K. Guo, Y. Guo, G. Fodor, and G. Ascheid, ”Uplink power control with MMSE receiver in multi-cell MU-massive-MIMO systems,” *IEEE International Conference on Communications (ICC)*, pages 5184 - 5190, Year 2014.

[45] P. C. Weeraddana, M. Codreanu, M. Latva-aho, and A. Ephremides, ”Resource Allocation for Cross-Layer Utility Maximization in Wireless Networks,” *IEEE Transactions on Vehicular Technology*, volume 60, pages 2790-2809, Jul 2011.

[46] M. Avriel, and A. C. Williams, ”Complementary geometric programming,” *SIAM Journal on applied Mathematics*, volume 19, pages 125-141, Jul 1970.

[47] Y. Zhang, and W.-P. Zhu, ”Energy-efficient pilot and data power allocation in massive multi-user multiple-input multiple-output communication systems,” *IET Communications*, volume 10, pages 1721-1729, Year 2016.

[48] S. Boyd, S. J. Kim, L. Vandenberghe, and A. Hassibi, ”A tutorial on geometric programming,” *Optimization and Engineering*, volume 8, pages 67-127, year 2007.

[49] M. Grant, S. Boyd, and Y. Ye, ”CVX: Matlab Software for Disciplined Convex Programming,” version 1.1, *online available: www.stanford.edu./boyd/cvx*, Nov 2007.

[50] E. L. Allgower, and K. Georg, ”Introduction to Numerical Continuation Methods,” *PA SIAM*, Philadelphia, year 2003.

[51] T. Marzetta, ”Noncooperative cellular wireless with unlimited numbers of base station antennas,” *IEEE Transactions on Wireless Communications*, volume 9, pages 3590-3600, Nov 2010.

[52] F. Rusek, D. Persson, B. K. Lau, E. G. Larsson, T. L. Marzetta, O. Edfors, and F. Tufvesson,” Scaling up MIMO: Opportunities and challenges with very large arrays,” *IEEE Signal Processing Magazine*, volume 30, pages 40-60, Jan 2013.

[53] S. M. Kay, ”Fundamentals of Statistical Signal Processing: Estimation Theory,” Upper

Saddle River , *NJ, USA: Prentice Hall*, 1993.

[54] W. Guo, and T. O'Farrell, "Relay deployment in cellular networks: Planning and optimization," *IEEE Journal on Selected Areas in Communications*, volume 30, pages 1597-1606, Sept 2012.

[55] H. Yang, and T. Marzetta, "Performance of conjugate and zero-forcing beamforming in large-scale antenna systems," *IEEE Journal on Selected Areas in Communications*, volume 31, pages 172-179, Feb 2013.

[56] M. Chiang, "Geometric programming for communication systems," *Foundations Trends Communication on Information Theory*, volume 2, pages 1-154, Jul 2005.

[57] S. Boyd, and L. Vandenberghe, "Convex Optimization," version 7, ISBN 0-521-83378-7, *online available: www.cambridge.org/9780521833783*, year 2009, .

[58] Z. Q. Luo, and W. Yu, "An introduction to convex optimization for communications and signal processing," *IEEE Journal on Selected Areas in Communication*, volume 24, pages 1426-1438, Aug 2006.

[59] M. R. Adhikari, "Basic Algebraic Topology and its Applications," DOI 10.1007/978-81-322-2843-1-2, *Springer India*, year 2016.

[60] W. Bryc, "Rotation invariant distributions," *Lecture Notes in Statistics*, volume 100, pages 51-69, year 1995.

[61] A. M. Tulino, and S. Verd, "Random matrix theory and wireless communications," *Foundations Trends Communication on Information Theory*, volume 1, pages 1-182, Jun 2004.

[62] "The MOSEK Optimization Tools Version 2.5. Users Manual and Reference," *Online Available: http://www.mosek.com*, year 2002.

[63] gpcvx, "A MATLAB Solver for Geometric Programs in Convex Form," *online available: http://www.stanford.edu/ boyd/ggplab/gpcvx.pdf*, Stanford University, Stanford, CA, year 2006.

[64] S. Boyd, "Sequential Convex Programming," *online available: http://www.stan ford.edu/class/ee364b/lectures/seq-slides.pdf*, year 2007.

[65] J.-H. Wui, D. Kim, "Resource Allocation for Collaborative Secondary Usage of Interfering Multiple Access Primary Channel by a Selective Relay," *IEEE Communications Letters*, volume 18, pages 556 - 559, Year 2014.

[66] B. Amouri, K. Ghanem, and M. Kaddeche, ”Hybrid relay selection-based scheme for UWB BANs combining MB-OFDM and decode-and-forward cooperative architectures,” *Electronics Letters*, volume 52, pages 2017-2019, year 2016.

[67] Y. Zhang, L. Pang, F. Gong, G. Ren, X. Liang, B. Li, J. Dou, and J. Li, ”Maximizing Achievable Rate Strategies for Incremental-Relay Multi-carrier Transmission,” *IEEE Transactions on Vehicular Technology*, volume 65, pages 5820 - 5825, Year 2016.

[68] L. Wang, T. Ke, M. Song, Y. Wei, and Y. Teng, ”Research on secrecy capacity oriented relay selection for mobile cooperative networks,” *IEEE International Conference on Cloud Computing and Intelligence Systems*, Beijing, China, pages 443-447, Sep 2011.

[69] Y. Zou, J. Zhu, X. Wang, and L. Hanzo, ”A survey on wireless security: Technical challenges, recent advances, and future trends,” *IEEE Proceedings*, volume 104, pages 1727-1765, Sep 2016.